TÜRKİYE
FIRAT UNIVERSITY
GRADUATE SCHOOL OF NATURAL AND APPLIED SCIENCES

THEORETICAL SPECTROSCOPIC PROPERTIES AND MOLECULAR DOCKING OF PLATINUM COMPLEXES

Hunar HAMA KHALID

Master's Thesis

Department of Physics

Program: Molecular Physics

JULY 2020

TÜRKİYE
FIRAT UNIVERSITY
GRADUATE SCHOOL OF NATURAL AND APPLIED SCIENCES

Department of Physics

Master's Thesis

THEORETICAL SPECTROSCOPIC PROPERTIES AND MOLECULAR DOCKING OF PLATINUM COMPLEXES

Author
Hunar HAMA KHALID

Supervisor
Prof. Dr. Niyazi BULUT

Co-Supervisor
Assoc. Prof. Dr. Sultan ERKAN

JULY 2020
ELAZIĞ

TÜRKİYE

FIRAT UNIVERSITY

GRADUATE SCHOOL OF NATURAL AND APPLIED SCIENCES

Department of Physics

Master's Thesis

Title: Theoretical Spectroscopic Properties and Molecular Docking of Platinum Complexes

Author: Hunar HAMA KHALID

First Delivery Date: 10/06/2020

Defense Date: 07/07/2020

THESIS APPROVAL

This thesis, which was prepared according to the thesis writing rules of the Graduate School of Natural and Applied Sciences, Fırat University, was evaluated by the committee members who have signed the following signatures and was unanimously approved after the defense exam made open to the academic audience.

Signature

Danışman: Prof. Dr. Niyazi BULUT
Firat University, Faculty of Science

Second supervisor: Assoc. Prof. Dr. Sultan ERKAN
Cumhuriyet University, Faculty of Science

President: Prof. Dr. Sinan AKPINAR
Firat University, Faculty of Science

Member: Assoc. Prof. Dr. Ömer KAYĞILI
Firat University, Faculty of Science

Member: Assoc. Prof. Dr. Bayram GÜNDÜZ
Malatya Turgut Özal University, Faculty of Science

This thesis was registered at the meeting of the Board of Directors of the Institute on ..... / ..... / 20 .....

Signature

Prof. Dr. Soner ÖZGEN
director of Graduate School

DECLARATION

I hereby declare that I wrote this Master's Thesis titled "Theoretical Spectroscopic Properties and Molecular Docking of Platinum Complexes" in consistent with the thesis writing guide of the Graduate School of Natural and Applied Sciences, Firat University. I also declare that all information in it is correct, that I acted according to scientific ethics in producing and presenting the findings, cited all the references I used, express all institutions or organizations or persons who supported the thesis financially. I have never used the data and information I provide here in order to get a degree in any way.

7 July 2020

Hunar HAMA KHALID

PREFACE

Platinum complexes, which are important with their anti-cancer properties were docked with molecular simulation against breast, ovarian, colon, pancreatic, lung, and melanoma cancer cell lines. The investigated complexes showed the highest inhibitory activity against the breast cancer cell line. We concluded that, after evaluating all theoretical results, the title complexes can be considered as an anticancer drug. Finally, the investigated complexes found to be a good candidate for ETL, HTL, and HIL material.

First of all, I would like to say my appreciation to the Almighty Allah, for his support, generosity and help us to complete my research. I really appreciate that both of my supervisor's reviewed my thesis and they corrected some mistakes about information. So, I want to show my thankfulness and highest thankfulness to my first supervisor's Prof. Dr. Niyazi BULUT, and my second supervisor's Assoc. Prof. Dr. Sultan ERKAN for all the support and patience that helped me to overcome my problems and their leadership on the right path during my work without him, it would unbelievable to me to accomplish this research. Finally, I want to thank my friend M. Hanifi KEBIROGLU's contribution.

Hunar HAMA KHALID
Elazığ, 2020

TABLE OF CONTENTS

Page

PREFACE iv

TABLE OF CONTENTS v

ABSTRACT vii

ÖZET viii

LIST OF FIGURES ix

LIST OF TABLES x

1. INTRODUCTION 1

1.1. Platinum Complexes on Cancer Therapy 1

1.2. Photodynamic Therapy 2

1.2.1. Platinum Complexes on Photodynamic Therapy 2

1.3. Photochemistry and Luminescence 3

1.3.1. Luminescence Properties of Platinum Complexes 3

1.4. OLED Properties 4

1.5. Computational Chemistry 5

1.5.1. Optimized Structure 5

1.5.2. Computational Spectroscopy 5

1.5.3. Molecular Electrostatic Potential (MEP) Maps 6

1.5.4. Theoretical OLED Properties 7

1.5.5. Drug Modeling 8

2. MATERIALS AND METHODS 10

2.1. Density Function Theory (DFT) 10

2.1.1. DFT Exchange-Correlation Functionals 11

2.2. Basis Sets 12

2.2.1. Minimal Basis Sets 13

2.2.2. Split-Valence Basis Sets 13

2.2.3. Correlation-Consistent Basis Sets 14

2.3. Molecular Docking 14

2.3.1. Hex Docking Program 15

2.4. Aim 16

3. RESULTS AND DISCUSSION 18

3.1. Optimized Structures 20

3.2. FT-IR Spectra and Vibrational Assignments 21

3.2.1. C-H Bond Stretching 23

3.2.2. C=C, C-C Bond Stretching Vibrations 23

3.2.3. C=N, C-N Bond Stretching 24

3.3. ^{13}C-NMR Spectra 24

3.4. Molecular Electrostatic Potential (MEP) Surface 26

3.5. Molecular Docking Study 27

3.6. OLED Properties 32
4. CONCLUSIONS 36
REFERENCES 37
CURRICULUM VITAE

ABSTRACT

Theoretical Spectroscopic Properties and Molecular Docking of Platinum Complexes

Hunar HAMA KHALID

Master's Thesis
FIRAT UNİVERSİTY
Graduate School of Natural and Applied Sciences

Department of Physics
July 2020, Page: x + 043

Vibrational bond stretching and Nuclear Magnetic Resonance (NMR) chemical shifts of Pt(dpb)Cl, Pt(Fdpb)Cl, Pt(F_2dpb)Cl, and Pt(dpb)I complexes have been investigated with computational chemistry methods. ^{1}H-NMR experimental data for Pt(dpb)I complex are compared with the proton chemical shifts values calculated by Hartree-Fock (HF) and Density Functional Theory (DFT) methods at a level of B3LYP and M062X functions with CEP-4G, CEP-31G, CEP-12G, LANL2DZ, LANL2MB, and SDD basis sets. Electrophilic and nucleophilic regions of the complexes were determined by molecular electrostatic potential (MEP). Experimental spectroscopic deficiencies, like infrared (IR) and ^{13}C-NMR, were predicted theoretically. In addition, molecular docking studies are applied against breast, lung, ovarian, pancreatic, and melanoma cancer cell lines. It was found that the complexes were active against investigated cancer cell lines except for pancreatic one as compared to the cis-platinum. Finally, OLED material properties of platinum complexes are investigated.

Keywords: Platinum complexes, FTIR and NMR, Molecular docking, Anti-Cancer

ÖZET

Platin Komplekslerinin Teorik Spektroskopik Özellikleri ve Moleküler Yerleştirme

Hunar HAMA KHALID

Yüksek Lisans Tezi

FIRAT ÜNİVERSİTESİ
Fen Bilimleri Enstitüsü

Fizik Anabilim Dalı
Temmuz 2020, Sayfa: x + 043

Hesaplamalı kimya yöntemleri ile Pt(dpb)Cl, Pt(Fdpb)Cl, Pt(F2dpb)Cl ve Pt(dpb)I komplekslerinin titreşim bağı gerilmesi ve Nükleer Manyetik Rezonans (NMR) kimyasal kaymaları araştırılmıştır. Pt(dpb)I kompleksi için 1H-NMR deneysel verileri, CEP-4G, CEP ile B3LYP ve M062X fonksiyonları ile Hartree-Fock (HF) ve Yoğunluk Fonksiyonel Teorisi (DFT) yöntemleri ile hesaplanan proton kimyasal kayma değerleri ile karşılaştırılıp CEP -31G, CEP-12G, LANL2DZ, LANL2MB ve SDD temel kümeleri kullanıldı. Komplekslerin elektrofilik ve nükleofilik bölgeleri moleküler elektrostatik potansiyel (MEP) ile belirlenmiştir. Kızılötesi (IR) ve ^{13}C-NMR gibi deneysel spektroskopik eksiklikler teorik olarak hesaplanmıştır. Ayrıca, göğüs, akciğer, yumurtalık, pankreas ve melanom kanseri hücre hatlarına karşı moleküler yerleştirme (docking) çalışmaları yapıldı. Komplekslerin, cis-platin ile karşılaştırıldığında pankreatik olanlar dışındaki araştırılmış kanser hücrelere karşı aktif oldukları bulundu. Son olarak, platin komplekslerinin OLED malzeme özellikleri araştırıldı.

Anahtar Kelimeler: Platin kompleksleri, FTIR ve NMR, Moleküler yerleştirme, Anti-Kanser

LIST OF FIGURES

Page

Figure 1.1 Different Coordinated Metal Complexes 1
Figure 1.2. Molecular Structure of Cisplatin and Carboplatin. 1
Figure 1.3. Some Complexes That Increase Cytotoxicity When Irradiated With UV. 2
Figure 1.4. Luminescent Platinum(II) Complexes 4
Figure 1.5. Layers of OLED Device 4
Figure 1.6. Optimized Structure Alq3 and TPD Reference Materials. 5
Figure 1.7. The Two-Dimension Electrostatic Potential Map of a Hypothetical Molecule. 7
Figure 1.8. MEP Map of a Platinum Complex 7
Figure 1.9. Binding Sites and Catalytic Site of a Protein. 9
Figure 2.1. Key-Lock Analogy Used in Docking Process. 15
Figure 2.2. Docking Result Obtained with Hex Program. 16
Figure 2.3. Structures of PlatinumCl, Pt(Fdpb)Cl, Pt(F2dpb)Cl, and PlatinumI. 17
Figure 3.1. Optimized Structures and Atomic Labeling for PlatinumI. 18
Figure 3.2. Optimized Structures for PlatinumCl, Pt(Fdpb)Cl, Pt(F_2dpb)Cl, and PlatinumI. 21
Figure 3.3. FT-IR Spectra of PlatinumCl, Pt(Fdpb)Cl, Pt(F_2dpb)Cl, and PlatinumI. 22
Figure 3.4. ^{13}C-NMR Spectra of Mentioned Complexes 24
Figure 3.5 The MEP Surface Maps For PlatinumCL, Pt(Fdpb)Cl, Pt(F_2dpb)Cl. 26
Figure 3.6. The Binding Modes of PlatinumCl, Pt(Fdpb)Cl, Pt(F2dpb)Cl, and PlatinumI with 1JNX 28
Figure 3.7. The binding modes of PlatinumCl, Pt(Fdpb)Cl, Pt(F_2dpb)Cl, and PlatinumI with 1X2J 29
Figure 3.8. The binding modes of PlatinumCl, Pt(Fdpb)Cl, Pt(F_2dpb)Cl, and PlatinumI with 2VFJ 29
Figure 3.9. The binding modes of PlatinumCl, Pt(Fdpb)Cl, Pt(F2dpb)Cl, and PlatinumI with 4J80. 30
Figure 3.10. The binding modes of PlatinumCl, Pt(Fdpb)Cl, Pt(F2dpb)Cl, and PlatinumI with 4ZQK. 30

LIST OF TABLES

Page

Table 3.1. ^{1}H-NMR chemical shift values (GIAO/HF) method in the gas phase for PlatinumI 18
Table 3.2. ^{1}H-NMR chemical shift values (GIAO/B3LYP) method in the gas phase for PlatinumI 19
Table 3.3. ^{1}H-NMR chemical shift values (GIAO/M062X) method in the gas phase for PlatinumI 19
Table 3.4. Regression coefficients (R^2) and experimental values for chemical shifts of ^{1}H-NMR.....20
Table 3.5. Vibrational frequencies of PlatinumCl, Pt(Fdpb)Cl, Pt(F_2dpb)Cl, and PlatinumI 22
Table 3.6. Chemical shift values of carbon atoms in mentioned complexes.....25
Table 3.7. The interaction energies (kcal/mol) between studied proteins and the selected target proteins ...27
Table 3.8. The interaction modes between studied ligand and the selected 1JNX.....31
Table 3.9. The interaction modes between studied ligand and the selected 2VFJ 31
Table 3.10. The interaction modes between studied ligand and the selected 1X2J.....32
Table 3.11. The interaction modes between studied ligand and the selected 4J80 32
Table 3.12. The interaction modes between studied ligand and the selected 4ZQK.....32
Table 3.13. The adiabatic and (IPa/IPv) and (EAa/EAv) (in eV) for the platinum complexes 35

1. INTRODUCTION

Cancer is an abnormal or uncontrolled growth of new cells anywhere on the body. Cancer cells invade the surrounding tissues and can metastasize to body parts. Cancer cells are formed by mutant gene formation in cell DNA. There are many methods of treating such a condition that causes cell DNA to mutate. Among these methods, the place of chemical therapy (chemotherapy) is very important. It is known that many organic and inorganic chemical species are used for this purpose. Inorganic chemical species are very popular in cancer treatment in recent years. The fact that metal complexes have different coordination numbers (Figure 1.1) and different redox properties facilitated the development of metal complexes medically.

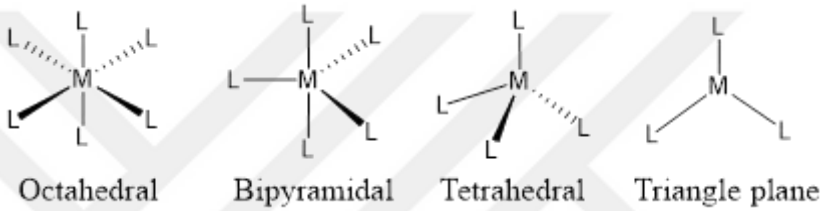

Figure 1.1. Different Coordinated Metal Complexes [1].

Negative portions of proteins and nucleic acids provide excellent ligands for binding to positively charged metal centers. Thus, positive results are obtained in cancer treatment by repairing the mutant parts of DNA.

1.1. Platinum Complexes on Cancer Therapy

In the last thirty years, platinum-based drugs, especially cisplatin and carboplatin are given Figure 1.2, have dominated the treatment of various cancers. Platinum complexes with cis geometry inhibit the growth of cancer cells according to structure-activity relationships.

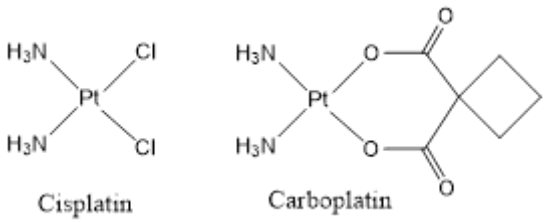

Figure 1.2. Molecular Structure of Cisplatin and Carboplatin [4]

These complexes have at least one N-H group responsible for the hydrogen bond, donor properties, important for the biological target. Platinum complexes are popular chemotherapeutic

agents due to ligand exchange kinetics. The ligand exchange behavior of Platinum complexes is rather slow, which provides high kinetic stability. In this way, platinum complexes can be classified as the most functional agent used in chemotherapy and photodynamic therapy (PDT), one of the notable methods of cancer treatment.

1.2. Photodynamic Therapy

Photodynamic therapy (PDT) is a treatment in which photosensitive substance is used. When light is exposed to a certain wavelength of light, they produce an oxygen form that kills close cells [2-4]. Each photosensitive substance is activated by light at a certain wavelength [4,5]. This wavelength determines how far light can travel in the body [4,6]. Therefore, they use certain photosensitizers and light wavelengths to treat different parts of the body with PDT. The first step in the use of PDT for cancer treatment is a photosensitizing agent injected into the bloodstream [2] and the agent leaves most normal cells, but the tumor is exposed to light and light destroys most cancer cells [2-4,7].

1.2.1. Platinum Complexes on Photodynamic Therapy

Photodynamic therapy (PDT) is one of the new methods developed to kill cancer cells. In this treatment, it is a treatment that uses special drugs called light-sensitive agents with light. Phototherapy with photodynamic therapy (PDT) and photoactive chemotherapy (PACT) has received much attention in the treatment of cancer due to its minimal invasiveness [8].

Photoactive platinum complexes have Pt (II) with d^8 electron configuration and Pt (IV) with d^6 electron configuration. Pt (II) complexes have been studied for blocking the growth of cancerous cells on different types of human cancer [9]. Because Pt (II) complexes have a wide emission color spectrum. They also have several distinctive features, such as high luminescence, short life of triple excited states. Different platinum complexes made with trans-platinum are given in Figure 1.3. [10].

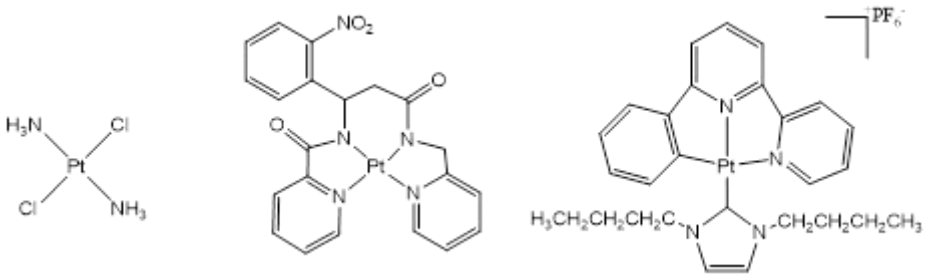

Figure 1.3. Some Complexes That Increase Cytotoxicity When Irradiated With UV [13]

When the complexes are given in Figure 1.3. were irradiated with UVA, they showed a double increase in toxicity compared to trans-platinum. The increase in cytotoxicity was associated with the formation of bifunctional DNA interstream cross-links that could not occur in the dark.

Platinum-DNA interaction was first enlightened by Roberts and Pascoe. This form of interaction applies to all metal complexes. Platinum complexes interact with DNA, and with this interaction, a twist of 35-40 ° occurs in the structure of DNA [11-13]. Thus, DNA polymerase is prevented and cancerous cell/tissue death occurs [14,15]. Medicines containing platinum form an active hydrolysis product. It also interacts with serum proteins or sulfur-containing amino acids/peptides. In this way, it makes proteins and amino acids inactive. As a result, platinum complexes form a coordination compound with DNA [16,17].

1.3. Photochemistry and Luminescence

Photochemistry is a sub-branch of chemistry related to the chemical effects of light. This term generally is used to describe chemical reactions that accord by absorption of ultraviolet-visible light or infrared radiation [18].

Luminescence can be defined as the energy absorbed by material from an external source and reemits this energy in the form of visible band light. The external energy source can come from many sources, including chemical, biological, and physical. If this source is based on radiology, this event is called photoluminescence. Luminescence is divided into two [19].

- Fluorescence, which is (more or less) the instantaneous emission of light
- Phosphorescence, which describes delayed light emission

1.3.1. Luminescence Properties of Platinum Complexes

Organometallic complexes, such as platinum (Pt) complexes, attracted great interest in both basic and applied research areas. For example, it has application areas such as chemical sensors and photocatalysts [20-23]. It is also highly effective in organic light-emitting diodes (OLEDs) thanks to the high internal quantum efficiency of organometallic complexes. This is because it has a strong spin-orbital pairing at room temperature (RT) [24-26]. Its emission wavelength and luminescence efficiency are due to the fact that the complex ligand affects the molecular atomic d-orbitals. Therefore, it is valuable to investigate the crystal structures and photophysical properties of organometallic complexes [27-30]. Most platinum complexes have developed around luminescent Pt (II) complexes that have been explored for their beneficial photophysical properties. Their high

efficiency and long life of the emitter state have enabled such complexes to be used in applications such as chemosensors photocatalysis light-emitting diodes and photovoltaic devices. In particular, the square planar Pt (II) complexes and ligands that provide π delocalization provide unmatched shine [31-34]. The platinum complexes given in Figure 1.4. are highly efficient OLED compounds that have been studied in recent years.

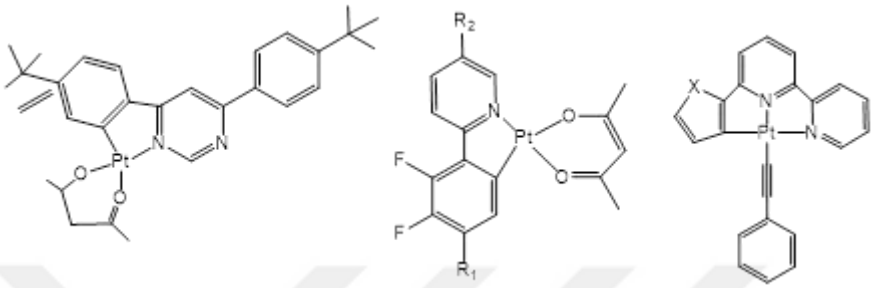

Figure 1.4. Luminescent Platinum(II) Complexes [32-34].

1.4. OLED Properties

The organic compound's ability to light-emitting after organic electroluminescence is called OLED or Organic LED [35,36]. An OLED device occurs of an electron transport layer (ETL), an emitter layer (EL), and a hole transport layer (HTL) between a cathode and an anode [37-39]. Besides these layers, next to the cathode is the electron injection layer (EIL) and the anode's hole injection layer (HIL) [40,41]. These layers are shown in Figure 1.5. [42].

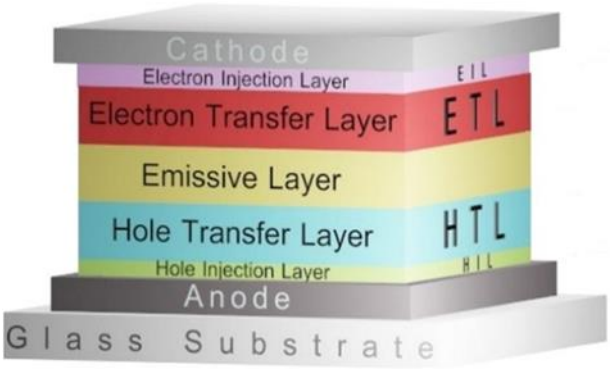

Figure 1.5. Layers of OLED Device [42]

In order to produce highly efficient OLED devices, two important reference materials are considered for the design of an electron transport layer (ETL) and a hole transport layer (HTL) materials. Typical material for ETL compounds is tris(8-hydroxyquinoline) aluminum complex (Alq3) [43-45]. Typical material for HTL compounds is N, N'-diphenyl-N, N'-bis (3-

methylphenyl)-1,1′-diphenyl-4,4′-diamine (TPD) [46-48]. The molecular structures of Alq3 and TPD compounds are given in Figure 1.6.

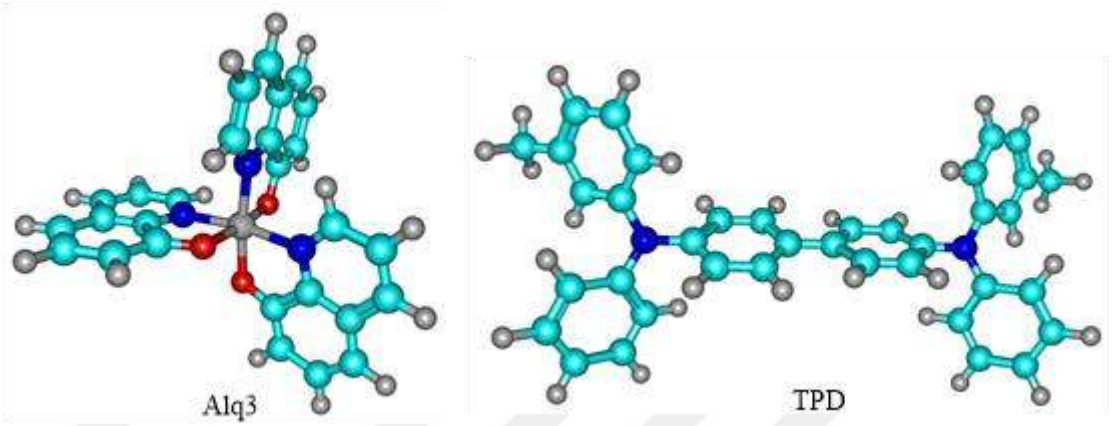

Figure 1.6. Optimized Structure Alq3 and TPD Reference Materials [46]

1.5. Computational Chemistry

Computational chemistry is an important tool used as a combination of computer technology and theoretical chemistry. Computational chemistry methods have many advantages, such as reducing experimental costs and reducing time loss. Moreover, computational chemistry methods can analyze three-dimensional structures, spectroscopic properties, anti-cancer activities depending on the molecular structure and the molecular properties such as OLED properties.

1.5.1. Optimized Structure

In computational chemistry, the position on the geometry optimization potential energy surface (PES) is a fixed point. That is, according to the molecule chemical binding model, the atomic force on each atom is acceptably close to zero.

1.5.2. Computational Spectroscopy

Computational chemistry can calculate the spectra of the compounds for a proposed compound to see if the original frequencies and frequency shifts in the model match the observation. Typically, frequencies are calculated more accurately than experimental because frequencies are a function of the square root of the force constant. However, quantum methods can effectively determine relative IR and Raman densities that are useful for assigning structures to vibration spectra [48]. However, frequencies are generally scaled to a predetermined factor that

takes into account the basic set, electron correlation, and a harmonic effect [49, 50]. Vibration frequencies are calculated analytically with the following equations:

$$V_{ij} = \frac{1}{\sqrt{m_i m_j}}\left(\frac{\partial^2 V}{\partial_{qi}\partial_{qj}}\right) \quad (1.1)$$

where V_{ij} is the Hessian matrix, m_i is the mass of atom i, and ∂_{qi} refers to the displacement of the atom i in the x-, y- or z-direction.

Nuclear magnetic resonance (NMR) spectroscopy is not a highly sensitive technique in molecular structure determination. Because NMR allows identifying the elements around the element. Two- and three-dimensional techniques enable the further development of structures that are particularly important for determining the structure of organic and inorganic molecules [51-53].

The most typical NMR parameter calculated is the chemical shift of a particularly related nucleus. The location of the signals in the NMR spectrum is determined by comparison with a reference standard substance, and TMS (tetramethylsilane) is usually used for this. The gauge-including atomic orbital (GIAO) method containing meters is the most widely used [54, 55]. It uses basis functions that have an explicit field dependence in the GIAO method.

1.5.3. Molecular Electrostatic Potential (MEP) Maps

Electrostatic potential maps describe a three-dimensional picture of molecules. These maps allow someone to visualize the charge distribution in a molecule. Charge distributions in a molecule can be used for determining how any molecules interact with each other. A very specific data of the molecule is obtained with the electrostatic potential map. The electrostatic potential energy at a certain distance from the nucleus of the molecule is calculated by computer programs. This electrostatic potential is a measure of the power of nuclei and electrons at a given location. A hypothetical electrostatic potential map of a mine is provided in Figure 1.7. However, when considered in two dimensions, this may seem rather meaningless.

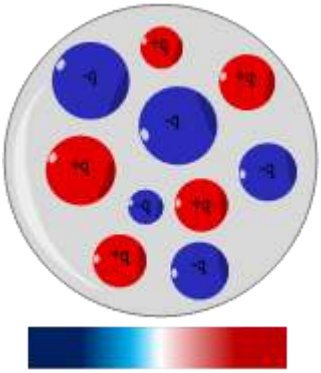

Figure 1.7. The Two-Dimension Electrostatic Potential Map of a Hypothetical Molecule [51].

The hypothetical molecule can be two-dimensional, but molecules are three-dimensional. For this reason, computer programs also take into account the three-dimensional is surface calculations of molecules. MEP maps define the electrophilic and nucleophilic regions of molecules. It also determines the chemical bonding regions of the molecule. Figure 1.8 shows the MEP map for a platinum complex.

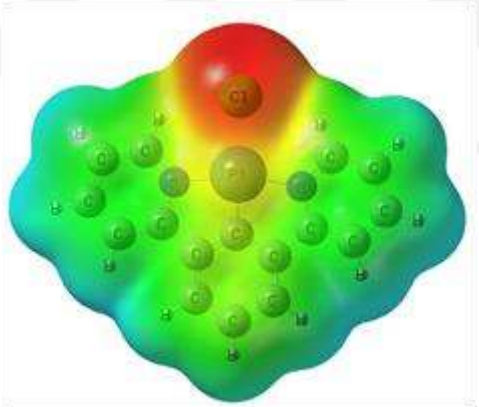

Figure 1.8. MEP Map of a Platinum Complex [54]

It is very easy to interpret and understand the differences in electrostatic potential energy with a color-coded map. Red areas with low potential are characterized by abundant electrons. It is characterized by high potential, blue areas, relative electron absence.

1.5.4. Theoretical OLED Properties

Understanding the charge-carrying system of light-emitting diodes (OLEDs) is very important for their correct use and development. Marcus theory applications are quite useful for computational chemistry methods. The theory of Marcus was proposed by Rudolph A. Marcus in 1956 [56]. With this theory, the rate of electron transfer reactions can be explained by the movement

of an electron in the transition from electron donor chemical type to electron acceptor chemical type.

$$K_{ij} = \frac{4\pi^2}{h} H_{ij} \frac{1}{\sqrt{4\pi\lambda k_B T}} exp\left[-\frac{(\lambda+\Delta G_{ij})^2}{4\lambda k_B T}\right] \quad (1.2)$$

Here, H_{ij} is the electronic coupling between molecule i and j. In addition, this parameter represents charge transfer integral (*t*). ΔG_{ij} is the Gibbs difference free energy between the charge transfer from molecule i to j. λ is defined as reorganization energy, h, as usual, is Planck constant, k_B is Boltzmann constant, and T is defined as absolute temperature [57].

In explaining the OLED properties of molecules with computational chemistry methods, two basic parameters are examined. These are charge transfer integral and reorganization energy.

Charge transfer is crucial in understanding the charge-bearing property of the molecule in a chemical reaction [58]. The charge-carrying feature usually takes place between the π-systems of the molecule [59,60].

The reorganization energy is used to investigate the evolution of molecular geometry [61]. The area of action of the geometric deformation inside the molecule and the activity of the action force can provide important results. That is why the energy of the molecules undergoing restructuring is calculated.

1.5.5. Drug Modeling

In recent years, drug modeling studies have attracted great interest. The most important reasons for this interest in modeling studies are that they are not quite costly and time-consuming. Molecular modeling is based on the investigation of the relationship between the studied molecules with effect mechanism. This process is carried out in a 3D dimensional computer environment. All processes taking this basic principle into account are called molecular docking. In the molecular docking study, the chemical species is the ligand, and the effect factor is called the target protein. Ligands are organic and inorganic chemical species. The design of the synthesized or possibly to be synthesized ligands depends entirely on the user. The functional groups in ligands can be improved by the exchange of electron acceptor or electron donor groups. The activity of synthesized or designed ligands may vary depending on the interaction potency with target proteins. With the ligand examined, the target protein should form a key-lock model and have low binding energy. This is very important in determining the effectiveness of the ligand in theory. Therefore, the target

proteins to which the ligands will act are the utmost importance. Proteins are dynamic molecules whose functions vary according to their interaction. A protein may have active sites for more than one ligand as shown in Figure 1.9. [62].

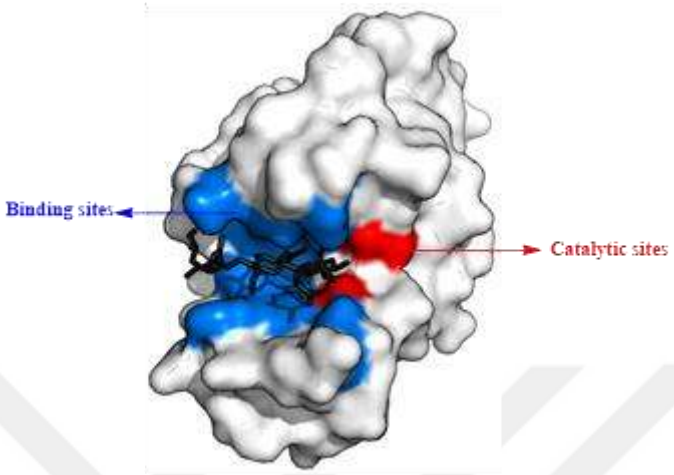

Figure 1.9. Binding Sites and Catalytic Site of a Protein [62].

A protein has more than one active site. The ligand interacts with one of these active regions. It is possible to determine the position of the ligands on the protein due to their binding poses. The forces that keep tens of thousands of atoms in the protein together are secondary chemical interactions such as van der Walls, hydrogen bond, hydrophobic interactions, polar interactions. Interactions between proteins and ligands are secondary chemical interactions. Interestingly, through these specific interactions, proteins can separate the ligand from thousands of molecules. Creating a protein crystal structure and visualizing it in 3 dimensions is a branch of separate science and is a very important science. There are quite different protein structures for each cancer cell, bacterial, and fungal cell. The appropriate target protein is determined and this target protein is supplied from the protein data bank. There are many programs in molecular docking.

2. MATERIALS AND METHODS

After the quantum theory was developed, quantum mechanical laws began to be applied to atoms and molecules. In this way, all the chemical properties of a molecule can be calculated by quantum theory. Thanks to the calculated chemical properties, experimental studies can be supported or they can predict the results obtained without performing experimental studies. The DFT method (B3LYP and M062X) and CEP-4G, CEP-31G, CEP-12G, LANL2DZ, LANL2MB, and SDD basis sets were used for the calculations made in this study.

2.1. Density Function Theory (DFT)

Density function theory is a theory developed by Thomas and Fermi in 1927. The DFT approach is based on modeling electron correlation through electron density functions. Such methods are based on the Hohenberg-Kohn theorem.

Hohenberg and Kohn developed the DFT in 1964 to find the status of an inhomogeneous electron gas system at minimum energy [64]. According to the Hohenberg-Kohn theorem, the ground state properties of a multi-electron system depend only on the electronic density of n(x, y, z). A system's total energy is expressed by E[n(x, y, z)]. Approximate functionalities used by DFT methods divide electronic energy into various parts [65].

$$E = E_T + E_V + E_J + E_{XC} \tag{2.1}$$

Here, the term kinetic energy resulting from the movement of E_T electrons is the term that defines the probe potential energy between the E_V core-electron attraction and nucleus pairs. E_J is the term electron-electron repulsion and E_{XC} is the exchange-correlation term that includes other electron-electron interactions. All terms, except nuclei-nucleus repulsions, are a function of the electron density ρ. Therefore, it is expressed functionally.

Hohenberg and Kohn showed that E_{XC} will be determined entirely by electron density. In general, in practice, the term E_{XC} was given only with an integral containing spin densities and possible components.

$$E^{XC} = \int f\left(\rho_\alpha(r), \rho_\beta(r), \nabla\rho_\alpha(r), \nabla\rho_\beta(r)\right) d^3r \tag{2.2}$$

Here ρ_α shows α spin density, ρ_β β spin density, and ρ total electron density ($\rho_\alpha + \rho_\beta$). E_{XC} is usually divided into two parts, the exchange and correlation sections corresponding to the same-spin and mixed-spin interactions.

$$E_{XC}(\rho) = E_X(\rho) + E_C(\rho) \tag{2.3}$$

All three terms in this equation depend on electron density and are called functional exchanges and correlation functions that define the two terms to the right of the equation. Each component can have two different types. Local functionalities depend only on electron density ρ [66].

2.1.1. DFT Exchange-Correlation Functionals

- **Local density approach (LDA):** It depends only on the density at a given point.
- **Gradient corrected approach (GGA):** Depends on local density and gradient.
- **Meta-GGA:** The functional density depends on its gradient and its second derivative.
- **Hybrid DFT:** Contains a trade term as part of the Hartree-Fock theory formulation [67].

In practice, self-compliant Kohn-Sam DFT calculations are made with an iterative procedure similar to SCF calculation. Kohn and Sam reported that such a similarity between the Hartree-Fock theory and DFT.

It contains a trade term as part of the Hartree-Fock theory formulation. Recently, Becke formulated functions that include a mixture of DFT exchange and HF as follows [68].

$$E_{hibrit}^{XC} = c_{HF}E_{HF}^{X} + c_{DFT}E_{DFT}^{XC} \tag{2.4}$$

Here, c's are constants. For example, a Becke-style three-parameter function can be defined by the following expression.

$$E_{B3LYP}^{XC} = E_{LDA}^{X} + c_0(E_{HF}^{X} - E_{LDA}^{X}) + c_X\Delta E_{B88}^{X} + E_{VWN3}^{C} + c_C(E_{LYP}^{C} - E_{VWN3}^{C}) \tag{2.5}$$

Here the parameter c0 is a constant that allows any mix of HF and LDA interchange. In addition, the cX parameter with Becke gradient correction is included in the LDA exchange. Similarly, the VWN3 local correlation function is used and this functional is optionally corrected by the parameter CC, which is the LYP correlation correction. In the B3LYP function, these parameter values are customized by Becke. Becke determined these parameter values as $c_0 = 0.20$, $cX = 0.72$ and $c_C = 0.81$ by optimizing first-order atomic energies in the atomization energy, ionization energy, proton affinity and G1 molecule set. Note that Becke's work uses Perdew-Wang's correlation function more than VWN3 and LYP.

Different functionalities can be created for LYP by replacing Perdew and Wang's 1991 gradient corrected correlation function in the same style by changing component functions and adjusting the values of the three parameters [66].

2.2. Basis Sets

The basis set used in computational chemistry is a set of functions which are called basis functions used to represent the electronic wave function in the Hartree-Fock method or density functional theory. The basis set can consist of atomic orbitals (which gives a linear combination of the atomic orbitals approach) or plane waves typically used in the solid-state community. That is, the mathematical representation of atomic orbitals in a molecular system is called basic sets. Molecular orbitals are derived from the linear composition of atomic orbitals. The wave functions of atomic orbitals are the product of radial and angular wave functions. Hydrogen-like orbitals, Slater type orbitals (STO), and Gaussian type orbitals (GTO) are the main functions for atomic orbitals. Ab initio calculations are made using STO or GTO, which is called the basis function [66]. Generally, basis sets for Ab initio or electronic structure calculations are created mostly from the GTO linear combination. In these functions, the angular part of the atomic orbitals is the same for GTO and STO. There is a difference only in the radial part.

The smallest basic sets are called minimal basic sets, which are used in each atom in the molecule uses a single base function for each orbit in the Hartree-Fock or DFT calculation on the free atom. For atoms such as Li, the basic functions of the p atom are added to the basic functions corresponding to the 1s and 2s orbitals of the free atom.

The minimal basis set is close to the exact value of the gas phase atom. In the next step, additional functions are added to describe the polarization of the electron density of the molecule in the atom. These are called polarization functions. This is very important for modeling chemical bonds because bonds are often polarized.

Another common addition to the basis sets is the addition of scattered functions. These are

the extended functions of Gauss with a small base that gives flexibility away from the nucleus to the "tail" part of the atomic orbitals. The diffuse basis functions are important for defining anions or dipole moments, but can also be important for the correct modeling of intermolecular and intermolecular bonds.

2.2.1. Minimal Basis Sets

They are basic sets that use a minimum number of basic functions for each atom in the molecule. The number of basic functions to be used for a molecule in minimal basic sets depends on the number of atoms in the molecule and the atomic orbital number. For example, the STO-3G foundation set is a minimal foundation set. The STO in this basic set indicates that Slater type orbitals are used as the basic function, and the term 3G uses three primitive Gaussian functions per basic function.

Commonly used minimal basis sets of this type are:

- STO-3G
- STO-4G
- STO-6G
- STO-3G* - Polarized version of STO-3G

2.2.2. Split-Valence Basis Sets

These are the basic sets that accept that the orbitals of the atoms in the molecule are not split, but that each valence orbital is split into two orbitals with different sizes. According to these basis sets, the shape of the orbital does not change, but its size changes.

Thus, the results obtained from the calculations are more accurate since the number of basic functions to be used increases. Basis sets such as 3-21G and 6-31G are split-valence foundation sets. Most are valence electrons that are mainly located in the bond during molecular bonding. Being aware of this fact, it is common to represent valence orbitals with more than one basic function (each may consist of a fixed linear combination of primitive Gauss functions in turn). Basic clusters with a large number of basic functions corresponding to each valence atom orbital are called basic clusters such as valence double, triple, quad-zeta, etc. [69].

A list of commonly used split-valence basis sets are:

- 3-21G
- 3-21G* - Polarization functions on heavy atoms

- 3-21G** - Polarization functions on heavy atoms and hydrogen
- 3-21+G - Diffuse functions on heavy-atom
- 3-21++G - Diffuse functions on heavy atoms and hydrogen
- 3-21+G* - Polarization and diffuse functions on heavy atoms
- 3-21+G** - Polarization functions on heavy atoms and hydrogen, as well as diffuse functions on heavy atoms
- 4-21G
- 4-31G
- 6-21G
- 6-31G
- 6-31G*
- 6-31+G*
- 6-31G(3df, 3pd)
- 6-311G
- 6-311G*
- 6-311+G*

2.2.3. Correlation-Consistent Basis Sets

These basis sets are developed by Dunning and coworkers designed for converging Post-Hartree–Fock calculations. They used empirical extrapolation techniques.

For first- and second-row atoms, the basis sets are cc-pVNZ where N=D, T, Q,5, 6... (D=double, T=triples, etc.). They include successively larger shells of polarization functions More recently these 'correlation-consistent polarized' basis sets have become widely used and are the current state of the art for correlated or post-Hartree–Fock calculations

2.3. Molecular Docking

Docking is a method used to estimate the preferred positions of atoms in space as a molecule forms a stable complex with another molecule. One of the key areas in which the docking method is used is to examine the nature of the possible drugs' binding to target molecules. Docking, which is a molecular mechanics method that has two types of applications: small molecule-protein and protein-protein docking; It is used to find the relationships between very large and biologically important molecules such as proteins, nucleic acids, and fats. ligand-protein docking (complex); considering that the ligand is free, the protein (receptor) is rigid and both the ligand and the protein

are flexible, it can be examined [70]. Docking steps are shown in Figure 2.1.

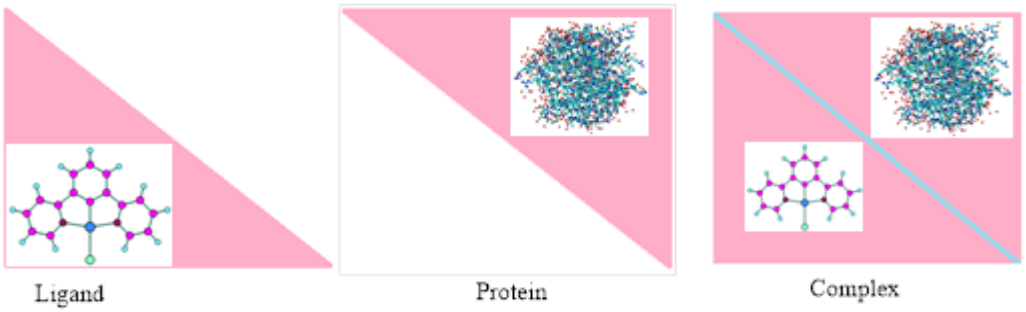

Figure 2.1. Key-Lock Analogy Used in Docking Process [70].

There are many docking programs available today. Hex 8.0.0 docking program is one of them.

2.3.1. Hex Docking Program

Hex is a program developed to calculate and display docking modes between the studied drug molecule (ligand) and the biological molecule (target protein). The Hex program uses spherical polar Fourier (SPF) collections in calculations. It binds ligand to protein in different poses to display and graph the minimum energy binding poses. It also provides fast results by using modern graphics processor units (GPUs).

In Hex's docking calculations, electrostatic charge and potential distribution are taken into account for the surface shape of each molecule. Considering these parameters, spherical pole basic functions are used in three-dimensional coordinates. The Hex program presents the coefficients vector of these parameters in their results, which are the combination of basic functions. It takes into account the steric density of van der Waals in the surface shapes of the proteins. After all, in this program, the basic principles of the classical electrostatic model are applied. Each time the complex interacts with the ligand, a docking score is obtained, which is a function of six degrees of freedom. This docking score gives the minimum interaction energy.

The calculations are applied to translation and rotation processes for the ligand and protein. The original expansion coefficients between this translation and rotation are calculated. Cartesian grid presentations are used with this approach. Using the fast Fourier transform (FFT) docking method, it performs docking correlations. The cartesian grid approach determines a docking station with only three translational degrees. The SPF approach speeds up the docking process. In addition, this approach allows calculating the original expansion coefficients of rotations and translations.

Hex is a pretty fast docking program. Because it uses FFT correlations as much as possible.

In addition, in the calculations, the FFT section ensures correct results with the help of GPU hardware. Thanks to its global polar approach, it uses six degrees of freedom and five Euler rotation angles. Thus, it presents the interaction energies that are formed as a result of the interaction of the ligand from different regions of the protein. In Figure 2.2, the drug is given by the interaction of a candidate platinum complex with a target protein representing lung cancer using the Hex program.

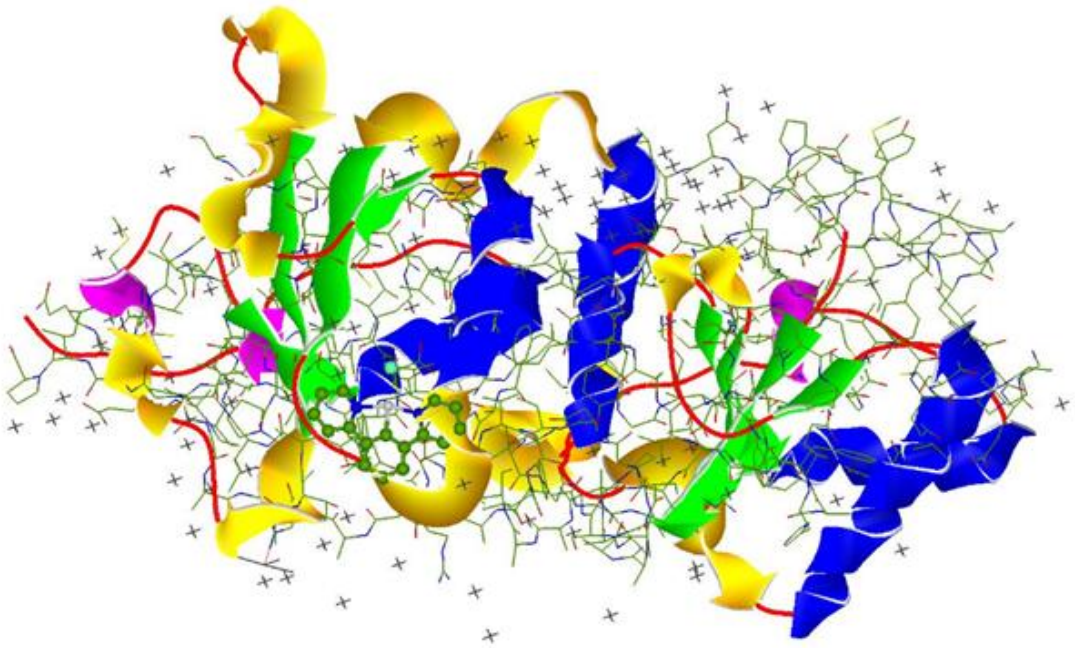

Figure 2.2. Docking Result Obtained with Hex Program.

2.4. Aim

Pt (II) complexes have been evaluated for cell growth inhibition against different human cancer cell lines [72]. It has been investigated that these complexes have a number of distinctive features, such as a wide emission color spectrum, high luminescence, short life of triple excited states [73]. Shinozaki et al. reported the effects of PlatinumCl (dpbH=1,3-di(2-pyridyl)benzene), Pt(Fdpb)Cl (FdpbH =4-fluoro-1,3-di(2-pyridyl)benzene), Pt(F_2dpb)Cl (F_2dpbH =4,6-difluoro-1,3-di(2-pyridyl)benzene) and PlatinumI on the excimer emission of the solvent and the substituent. From here on for simplicity and clarity Platinum will simply set as Platinum. In their study, they reported that the Pt (II) complex can exist not only as a blue-green donor as a monomer, but also as an excimer and trimer as a red and NIR donor. They also concluded that Pt (N ^ C ^ N) Cl could potentially be a perceived luminophore to report the lipid layer, micelle, live cell, and similar microenvironments [74]. In this study, spectroscopic and anticancer properties of Pt (II) complexes bearing a dpb ligand shown in Figure 2.3 are investigated depending on the molecular structure.

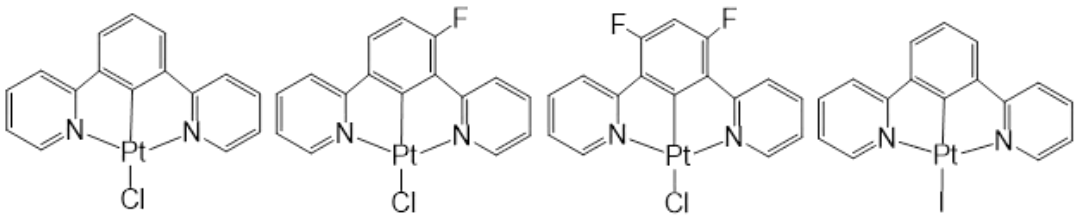

Figure 2.3. Structures of PlatinumCl, Pt(Fdpb)Cl, Pt(F2dpb)Cl, and PlatinumI.

PlatinumCl, Pt(Fdpb)Cl, Pt(F2dpb)Cl, and PlatinumI complexes have been investigated with computational chemistry methods. ^{1}H-NMR experimental data for the PlatinumI complex are compared with the proton chemical shifts values calculated by Hartree-Fock (HF) and Density Functional Theory (DFT) methods at a level of B3LYP and M062X functions with CEP-4G, CEP-31G, CEP-12G, LANL2DZ, LANL2MB, and SDD basis sets. Experimental spectroscopic deficiencies, like infrared (IR) and ^{13}C-NMR, were predicted theoretically. Electrophilic and nucleophilic regions of the complexes were determined by molecular electrostatic potential (MEP). In addition, molecular docking studies are applied against breast, lung, ovarian, pancreatic, and melanoma cancer cell lines. Molecular docking studies with HEX 8.0.0 simulation program against breast (PDB ID:1JNX), lung (PDB ID:1X2J), ovarian (PDB ID:2VFJ), pancreatic (PDB ID:4J80) and melanoma cancer (PDB ID:4ZQK) cell lines were performed for PlatinumCl, Pt(Fdpb)Cl, Pt(F_2dpb)Cl, and PlatinumI. Finally, it was found that the complexes were active against investigated cancer cell lines except for pancreatic one as compared to the cis-platinum.

3. RESULTS AND DISCUSSION

Before start to calculate any quantities with a computational chemistry method someone needs to optimize molecular structure with respect to energy minimizing. During that minimizing it is also important to obtain and interpret regression coefficients giving us some idea between theoretical deviation with respect to an experimental one.

For this purpose, HF, B3LYP, M062X methods and CEP-4G, CEP-31G, CEP-12G, LANL2DZ, LANL2MB, SDD basis sets, and proton chemical shift values were calculated for the PlatinumI complex. Firstly, the atomic labeling of the PlatinumI complex is given in Figure 3.1. Then, the calculated and the experimental ^{1}H-NMR chemical shift values for the PlatinumI complex are given in Table 3.1-3.3.

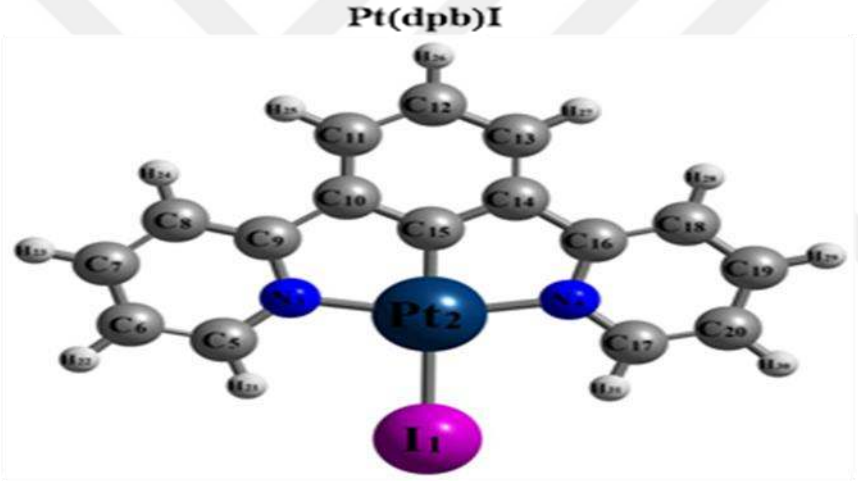

Figure 3.1. Optimized Structures and Atomic Labeling for PlatinumI.

Table 3.1. 1H-NMR chemical shift values (GIAO/HF) method in the gas phase for PlatinumI

Assign.	CEP-4G	CEP-31G	CEP-121G	LANL2DZ	LANL2MB	SDD	Exp.
21 H	11.13	10.29	10.35	10.92	9.95	9.91	9.83
22 H	9.77	8.17	7.86	8.19	7.77	7.20	8.18
23 H	10.49	8.91	8.86	9.07	8.39	8.08	7.48
24 H	10.15	8.60	8.32	8.46	8.01	7.47	8.05
25 H	10.17	8.87	8.58	8.70	7.97	7.67	7.71
26 H	9.32	8.69	7.91	8.05	7.61	6.99	7.38
27 H	8.37	8.87	8.58	8.70	7.97	7.67	7.71
28 H	10.15	8.60	8.32	8.46	8.01	7.47	8.05
29 H	10.49	8.91	8.86	9.07	8.39	8.08	7.48
30 H	9.77	8.17	7.86	8.18	7.77	7.20	8.18

Table 3.1. (Continue)

31 H	11.13	10.29	10.35	10.92	9.95	9.91	9.83
Ref.	31.08	33.40	33.45	33.66	33.11	33.66	-

$\delta=\Sigma_{H(references)}-\Sigma$, $\Sigma_{H(reference)\ (gaz)}$, Reference TMS

Table 3.2. 1H-NMR chemical shift values (GIAO/B3LYP) method in the gas phase for PlatinumI

Assign.	CEP-4G	CEP-31G	CEP-121G	LANL2DZ	LANL2MB	SDD	Exp.
21 H	10.41	10.26	10.15	-1.36	9.27	10.64	9.83
22 H	8.99	7.83	7.44	3.70	7.18	7.70	8.18
23 H	9.18	8.11	7.97	4.00	7.37	8.11	7.48
24 H	9.42	8.31	7.93	-0.74	7.35	7.99	8.05
25 H	9.22	8.25	7.88	3.03	7.09	7.94	7.71
26 H	8.56	7.67	7.39	1.69	6.83	7.46	7.38
27 H	9.22	8.25	7.88	3.03	7.09	7.94	7.71
28 H	9.42	8.31	7.93	-0.75	7.35	7.99	8.05
29 H	9.18	8.11	7.97	4.00	7.37	8.11	7.48
30 H	8.99	7.83	7.44	3.70	7.18	7.70	8.18
31 H	10.41	10.26	10.15	-1.36	9.27	10.64	9.83
Ref.	30.26	32.66	32.71	32.82	32.22	32.76	-

$\delta=\Sigma_{H(references)}-\Sigma$, $\Sigma_{H(reference)\ (gaz)}$, Reference TMS

Table 3.3. 1H-NMR chemical shift values (GIAO/M062X) method in the gas phase for PlatinumI

Assign.	CEP-4G	CEP-31G	CEP-121G	LANL2DZ	LANL2MB	SDD	Exp.
21 H	11.16	10.92	10.90	11.58	10.02	11.42	9.83
22 H	10.08	9.12	8.90	8.83	7.92	8.80	8.18
23 H	10.24	8.88	8.84	8.92	8.12	8.85	7.48
24 H	10.50	9.04	8.78	8.80	8.13	8.75	8.05
25 H	10.15	8.95	8.53	8.79	7.86	8.68	7.71
26 H	9.55	8.86	8.51	8.62	7.59	8.50	7.38
27 H	10.15	8.95	8.53	8.79	7.86	8.68	7.71
28 H	10.50	9.04	8.78	8.80	8.13	8.75	8.05
29 H	10.24	8.88	8.84	8.92	8.12	8.85	7.48
30 H	10.08	9.12	8.90	8.83	7.92	8.80	8.18
31 H	11.16	10.92	10.90	11.58	10.02	11.42	9.83
Ref.	30.53	32.78	32.91	32.96	32.58	32.88	-

$\delta=\Sigma_{H(references)}-\Sigma$, $\Sigma_{H(reference)\ (gaz)}$, Reference TMS

The regression coefficients results obtained with HF, B3LYP, M062X methods at CEP-4G, CEP-31G, CEP-12G, LANL2DZ, LANL2MB, SDD level of basis sets in comparison with the experimental data are listed in Table 3.4.

Table 3.4. Regression coefficients (R2) and experimental values for chemical shifts of 1H-NMR

Basis set	HF	B3LYP	M062X
CEP-4G	0.3821	0.8197	0.7701
CEP-31G	0.6038	0.8538	**0.9520**
CEP-121G	0.6224	0.8125	0.9206
LANL2DZ	0.7032	0.4877	0.8928
LANL2MB	0.7569	0.8918	0.8923
SDD	0.7080	0.8525	0.9028

These coefficients provide the ratio of the variance between one variable and the other. When R^2 values taken into account, it is closer to 1 for the M062X/CEP-31G level as can be seen in the last column of Table 4.4. This is one of the reasons chosen M062X/CEP-31G basis set for all rest of quantum calculations in this study. To interpret the proton chemical shift, tetramethylsilane (TMS) was taken as a reference. ^{1}H-NMR values of TMS was calculated for all methods and basis sets. The chemical shift for TMS proton was found to be 32.78 ppm at the M062X/CEP-31G level. Calculated chemical shift values for PlatinumI are 10.92, 9.12, 9.04, 8.95, 8.88, and 8.86 ppm and experimental values corresponding to the calculated chemical shifts are 9.83, 8.18, 8.05, 7.71, 7.48 and 7.38 ppm for PlatinumI complex [74].

3.1. Optimized Structures

The optimized structure of PlatinumCl, Pt(Fdpb)Cl, Pt(F_2dpb)Cl, and PlatinumI were depicted in Figure 3.2. The optimized structures were obtained at the most appropriate M062X/CEP31G level in the gas phase. Considering the geometry structure of all complexes, the tridentate 1,3-di(2-pyridyl) phenyl and halogen ligands formed a square planar geometry around the platinum as can be seen in Figure 3.2.

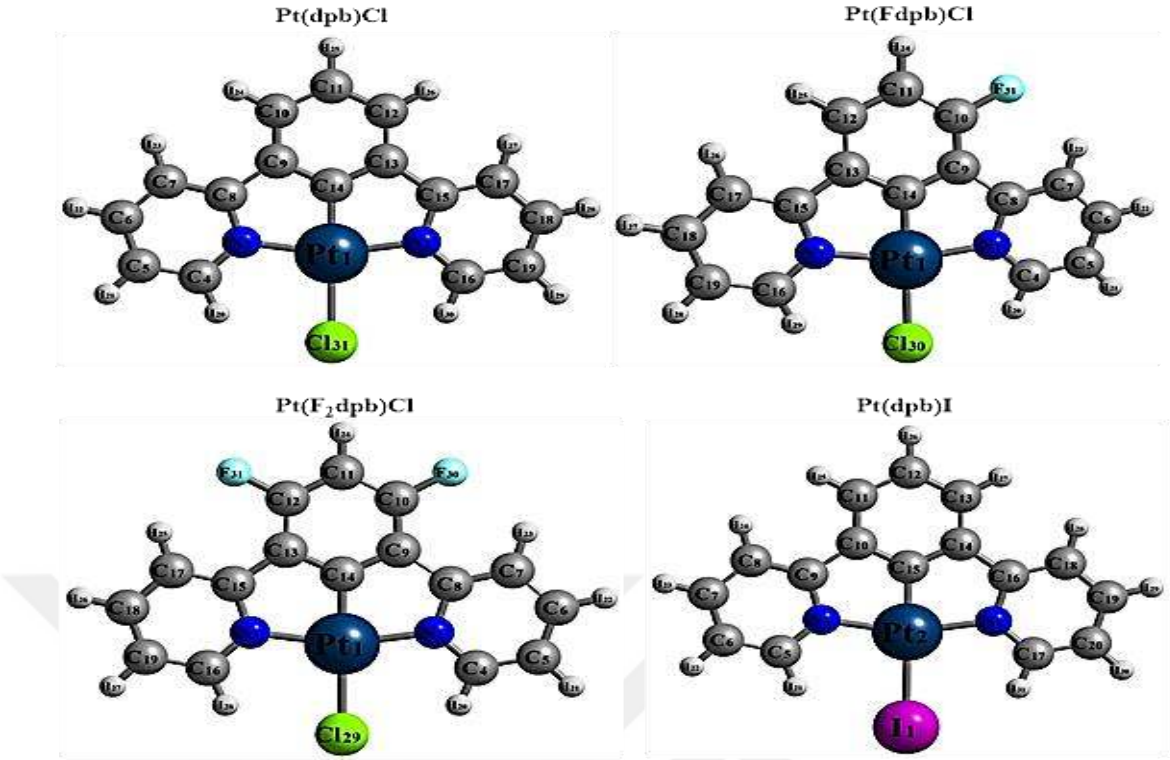

Figure 3.2. Optimized Structures for PlatinumCl, Pt(Fdpb)Cl, Pt(F2dpb)Cl, and PlatinumI.

3.2. FT-IR Spectra and Vibrational Assignments

FT-IR spectra is a very important technique in recognition of the skeletal structure of the investigated chemical species. For all complexes, harmonic frequencies were calculated at M062X/CEP-31G level. Theoretically simulated FTIR spectrum of the studied complexes is given in Figure 4.3. Bond stretching modes corresponding to the peaks in the IR spectrum of investigated platinum complexes are also given in Table 4.5. and C-H, C-C, C=C, C-N, and C=N bond stretching modes were evaluated in detail in the following subsection.

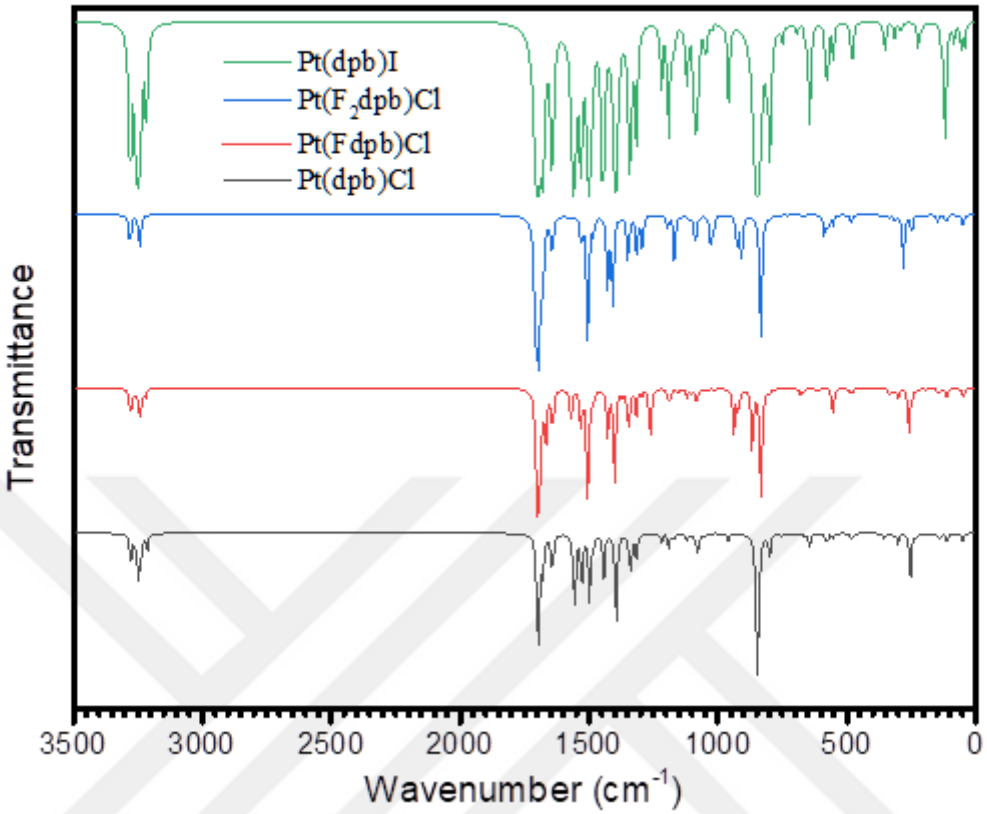

Figure 3.3. FT-IR Spectra of PlatinumCl, Pt(Fdpb)Cl, Pt(F2dpb)Cl, and PlatinumI

Table 3.5. Vibrational frequencies of PlatinumCl, Pt(Fdpb)Cl, Pt(F2dpb)Cl, and PlatinumI

Modes	PlatinumCl	Pt(Fdpb)Cl	Pt(F_2dpb)Cl	PlatinumI
ΓC-H	799 (vw)	833 (vs)	833 (vs)	798 (vw)
ΓC-H	846 (vs)	866 (m)	905 (vw)	847 (vs)
ΓC-H	958 (vw)	920 (vw)	926 (w)	958 (vw)
βC-H	1080 (vw)	1155 (vw)	1087 (w)	1086 (vw)
βC-H	1190 (vw)	1264 (m)	1168 (m)	1191 (vw)
βC-H	1314 (vw)	1344 (vw)	1293 (m)	1341 (w)
βC-H	1337 (vw)	1400 (s)	1407 (s)	1396 (s)
βC-H	1394 (s)	1506 (s)	1427 (m)	1445 (m)
βC-H	1498 (m)	1570 (w)	1505 (vs)	1499 (s)
βC-H	1555 (m)	1688 (m)	1677 (m)	1558 (m)
βC-H	1644 (vw)	1696 (vs)	1696 (vs)	1645 (vw)
βC-H	1696 (vs)	1701 (m)	1705 (vs)	1698 (vs)
νC-H	3214 (vw)	3222 (vw)	3242 (vw)	3209 (vw)
νC-H	3238 (vw)	3241 (vw)	3276 (vw)	3239 (vw)
νC-H	3247 (vw)	3275 (vw)	3281 (vw)	3248 (w)
νC-H	3278 (vw)	3283 (vw)	3282 (vw)	3279 (w)
νC=C	1314 (vw)	1316 (vw)	1315 (w)	1315 (vw)
νC=C	1394 (s)	1400 (s)	1407 (s)	1396 (s)

Table 3.5. (Continue)

νC=C	1442 (m)	1427 (m)	1427 (m)	1445 (m)
νC=C	1498 (m)	1570 (w)	1505 (vs)	1499 (s)
νC=C	1528 (m)	1639 (vw)	1641 (vw)	1531 (w)
νC=C	1555 (m)	1667 (m)	1677 (m)	1558 (m)
νC=C	1644 (vw)	1688 (m)	1691 (m)	1645 (vw)
νC=C	1678 (m)	1696 (vs)	1696 (vs)	1679 (w)
νC=C	1696 (vs)	1701 (m)	1705 (vs)	1698 (vs)
C-N	1314 (w)	1316 (vw)	1314 (w)	1315 (vw)
C=N	1639 (w)	1639 (vw)	1641 (vw)	1640 (vw)
C=N	1644 (w)	1645 (vw)	1646 (vw)	1645 (vw)

ν: Stretching, β: in-plane-bending, Γ: out-of-plane bending, vw: very week, w: week, m: medium, s: strong, vs: very strong.

3.2.1. C-H Bond Stretching

In aromatic compounds, stretching, in-plane bending and out of plane bending CH vibration modes can appear in 3100-3000 cm^{-1}, 1400-1000 cm^{-1}, and 1000-750 cm^{-1} ranges respectively [75, 76]. The stretching CH modes are generally appearing in a range of 3100- 3000 cm^{-1} with multiple soft bands and these bands may not be affected a whole nature of the substituent's [77-80]. The βC-H vibration modes show moderately sharp but not strong bands in the range 1100-1500 cm^{-1} and these bands are not so sensitive to the nature of substituents. The out of plane bending C-H deformation modes, in general, are in a range of 800-1000 cm-1 [78]. The C-H asymmetric stretching found in a position of 3080 cm^{-1} and the C-H symmetric stretching assigned to 3008, 2982 cm^{-1}. The tighter absorptions for aromatic compounds as can be in the (figure 4.3) occurs in the range of 900–650 cm^{-1} because of the C–H vibrations modes out of the plane to the aromatic ring [81-83]. In present work, the C-H stretching vibration mode is observed at about 3207-3278 cm^{-1} for PlatinumCl, 3222-3283 cm^{-1} for Pt(Fdpb)Cl, 3242-3282 cm^{-1} Pt(F_2dpb)Cl and 3209-3279 cm^{-1} PlatinumI which are reasonable a range of wavenumber with the literature. The C-H bending vibrations (in-plane and out-of-plane) are assigned at 1081-1696 cm^{-1}, 1155-1701 cm^{-1}, 1087-1705 cm^{-1}, and 1086-1698 cm^{-1} for PlatinumCl, Pt(Fdpb)Cl, Pt(F_2dpb)Cl, and PlatinumI, respectively and are listed in Table 3.5.

3.2.2. C=C, C-C Bond Stretching Vibrations

In general, C-C stretching vibrations modes in aromatic compounds can form a band in the estimation region of 1430–1650 cm^{-1} [84]. The ring of C-C stretching vibrations in Pyridine is reported in the literature as 1329-1431, 1420-1501, and 1419-1519 cm^{-1}, respectively [85, 86]. The

computed wavenumber for ν(C-C) modes falls between 1314-1696 cm^{-1}, 1316-1701 cm^{-1}, 1314-1705 cm^{-1}, 1315-1698 cm^{-1} for PlatinumCl, Pt(Fdpb)Cl, Pt(F_2dpb)Cl, and PlatinumI, respectively.

3.2.3. C=N, C-N Bond Stretching

One of the difficult tasks is to obtaining of C=N and C-N vibrations modes, for some mixing of vibrations can be possible in this region. C=N and C-N stretching vibrations appear in a range of 1670-1600 cm^{-1} and 1382-1266 cm^{-1} respectively [87]. The C=N and stretching vibrations of the title compounds lies at 1639, 1644 cm^{-1}, 1639, 1645 cm^{-1}, 1641, 1646 cm^{-1}, 1640, 1645 cm^{-1}, for PlatinumCl, Pt(Fdpb)Cl, Pt(F_2dpb)Cl, and PlatinumI, respectively.

3.3. ^{13}C-NMR Spectra

Nuclear magnetic resonance (NMR) is a popular technique to characterize any complex macromolecules [88]. DFT methods for calculations of magnetic shielding highly extends the size of molecules [89, 90]. Electronegative groups close to the system reduce the surrounding electron density, shielding of peak position from the external magnetic field, and moving the signal to higher ppm. Intermolecular effects can be examined by chemical shifts and this examination shows how electron density of neighboring groups influences the chemical shift observed for the complex molecule. A plotting comparative of calculated ^{13}C-NMR chemical shifts calculated at M062X/CEP-31G level of studied complexes is given in Figure 3.4. In addition, the calculated chemical shift values (δ_C) of carbons in the complexes are given in Table 3.6.

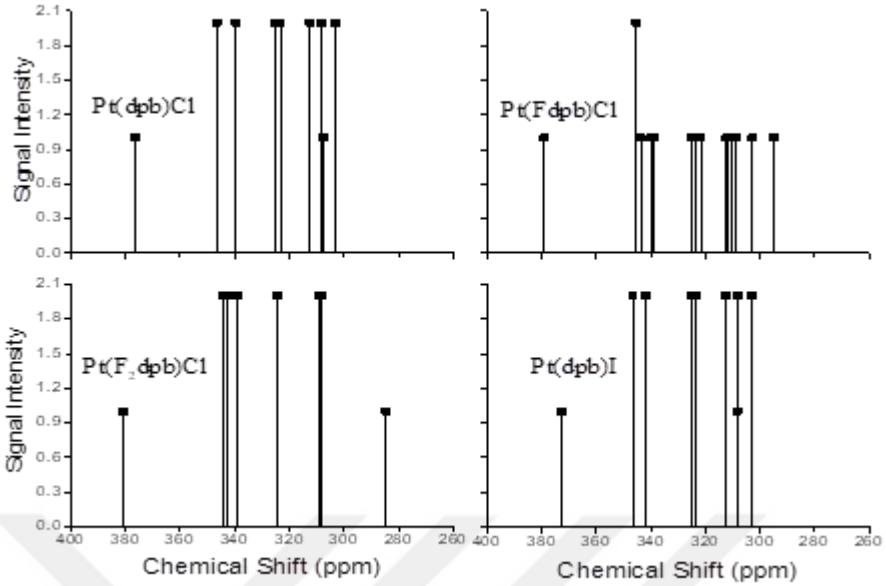

Figure 3.4. 13C-NMR Spectra of Mentioned Complexes

Table 3.6. Chemical shift values of carbon atoms in mentioned complexes

Pt(dpb)Cl		Pt(Fdpb)Cl		Pt(F_2dpb)Cl		Pt(dpb)I	
Atom	δ_{calc}	Atom	δ_{calc}	Atom	δ_{calc}	Atom	δ_{calc}
14-C	376	14-C	378	14-C	380	15-C	372
15-C	346	10-C	345	12-C	344	9-C	346
8-C	346	15-C	345	10-C	344	16-C	346
16-C	339	8-C	343	8-C	342	17-C	341
4-C	339	16-C	339	15-C	342	5-C	341
13-C	325	4-C	338	16-C	339	10-C	324
9-C	325	6-C	324	4-C	339	14-C	324
6-C	323	18-C	323	18-C	324	7-C	323
18-C	323	13-C	321	6-C	324	19-C	323
10-C	312	12-C	312	5-C	309	13-C	312
12-C	312	9-C	311	19-C	309	11-C	312
5-C	308	5-C	310	13-C	308	12-C	308
19-C	308	19-C	309	9-C	308	20-C	308
11-C	307	7-C	309	7-C	308	6-C	308
7-C	303	17-C	302	17-C	308	18-C	303
17-C	303	11-C	294	11-C	284	8-C	303

The ^{13}C NMR spectrum of considered molecules as can be seen from Figure 4.4 shows some sharp peaks corresponding to various carbon atoms because of the non-equivalence of the various carbon atoms. From Figure 3.4 one can notice that in PlatinumCl, Pt(F_2dpb)Cl, PlatinumI cases

there are almost intense peaks by overlapping peak positions, but in a case Pt(Fdpb)Cl it can be seen just one intense peak occurs because of losing symmetry of the system. The efficiency of the electronegative, however, is dependent upon far-near and direct-indirect interactions between the electronegative atoms and its neighboring carbons. The location of the peaks linked to the electronegative atom that attached to carbon atoms as can be seen in Table 3.6.

3.4. Molecular Electrostatic Potential (MEP) Surface

To have a deep interpretation of reactivity of any molecule, electrostatic potential calculations may give some advantage to evaluate the reactivity of molecules against positively or negatively charged reactants. Molecular electrostatic potential surface calculated and is depicted in Figure 3.5. In this figure, the high-density parts of the electrostatic potential energy values are colored with red and the lowest part is blue [91].

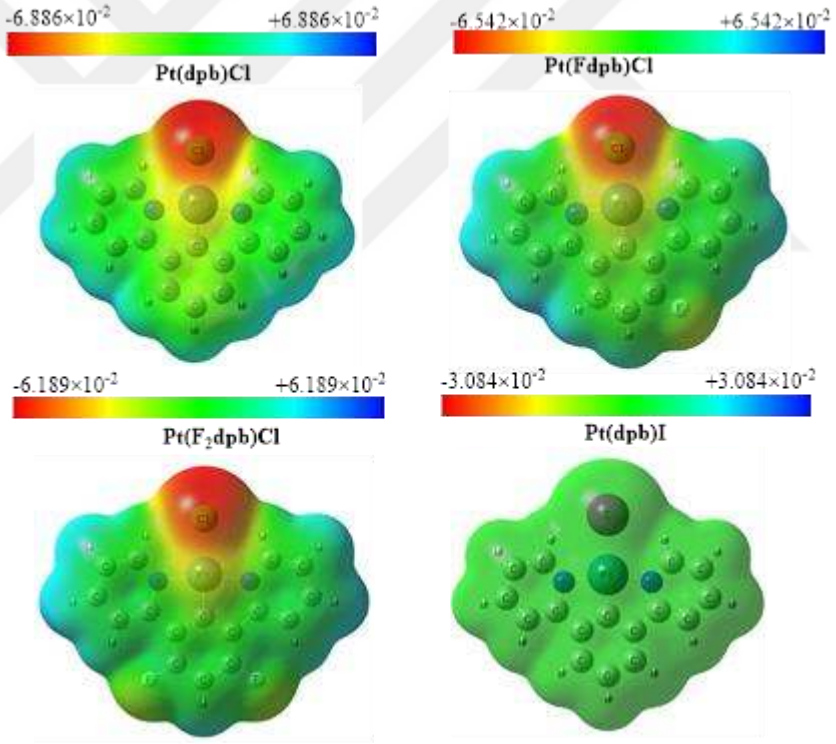

Figure 3.5. MEP Surface Maps For PlatinumCL, Pt(Fdpb)Cl, Pt(F2dpb)Cl and PlatinumI Complexes.

As can be seen from Figure 3.5., the active zones of the MEP, which is colored with red, of the complexes PlatinumCl, Pt(Fdpb)Cl, Pt(F_2dpb) Cl are the regions where the chlorine atom is located. When the ESP charge densities are examined, the ESP charge for PlatinumCl, Pt(Fdpb)Cl, Pt(F_2dpb)Cl are $\pm 6.886\times10^{-2}$, $\pm 6.542\times10^{-2}$ and $\pm 6.189\times10^{-2}$, respectively. The ESP charge density

for PlatinumI is $\pm 3.084 \times 10^{-2}$. This may show that the PlatinumI complex has an electropositive region. Considering these values and MEP figures one concludes that Chlorine complexes may interact with cancer cells more than iodine complexes. Also, MEP maps can be predicted from which region the complexes interact actively with cancer cells.

3.5. Molecular Docking Study

Platinum-based complexes are widely used in the treatment of almost all types of cancer such as breast, ovarian, colon, pancreatic, lung, melanoma. Molecular docking study for Pt(F_2dpb)Cl, Pt(Fdpb)Cl, PlatinumCl, and PlatinumI were performed with PDB ID:1JNX [92] (crystal structure of breast cancer-associated protein BRCT), PDB ID:1X2J [93] (the structural basis of defects in point mutations on the lung cancer), PDB ID:2VFJ [94] (structure of the A20 ovarian tumor domain), PDB ID:4J80 [95] (crystal structures of the multidomain cochaperone DnaJ on pancreatic cancer), PDB ID:4ZQK [96] (Structure of the complex of human programmed on the non-small cell lung cancer). Optimized structures of Pt(F_2dpb)Cl, Pt(Fdpb)Cl, PlatinumCl, and PlatinumI were transformed into pdb files with GaussView 6.0 program. 1JNX, 1X2J, 2VFJ, 4J80, and 4ZQK target proteins were procurement in the protein data bank. HEX 8.0.0 program was used to obtain the binding energies of related complexes with the target proteins. The binding energies between Pt(F_2dpb)Cl, Pt(Fdpb)Cl, PlatinumCl, and PlatinumI with 1JNX, 1X2J, 2VFJ, 4J80, and 4ZQK were given table 3.7.

Table 3.7. The interaction energies (kcal/mol) between studied proteins and the selected target proteins

Target protein	**PlatinumCl**	**Pt(Fdpb)Cl**	**Pt(F_2dpb)Cl**	**PlatinumI**	**Cis-Pt**
1JNX	-6.82	-7.14	-7.31	-6.84	-4.37
1X2J	-4.83	-4.77	-5.01	-4.89	-2.53
2VFJ	-0.48	-0.18	-0.89	-0.20	-1.78
4J80	-4.89	-4.83	-5.01	-5.04	-1.12
4ZQK	-4.54	-4.68	-4.81	-4.38	-3.14

Cis-platinum is a complex and widely used in cancer treatment. This complex, generally, is taken as a reference, and the efficacy of newly discovered platinum complexes is investigated for interaction energies of PlatinumCl, Pt(Fdpb)Cl, Pt(F_2dpb)Cl, PlatinumI and cis-Pt with 1JNX, 1X2J, 2VFJ, 4J80, and 4ZQK target proteins. As can be seen from the obtained data in Table 4.7, the binding affinity of Pt(F_2dpb)Cl, Pt(Fdpb)Cl, PlatinumCl, and PlatinumI to 1JNX, 1X2J and 4ZQK are higher than cis-Pt. Therefore, these complexes can be preferred to the cis-Pt complex in

breast and lung cancer treatment. The interaction energies of Pt(F_2dpb)Cl, Pt(Fdpb)Cl, PlatinumCl, and PlatinumI with 2VFJ target protein is smaller than the interaction energies of cis-Pt with 2VFJ. This indicates that these complexes' efficiency on the ovarian tumor may not as effective as cis-platinum. They investigated all complexes exhibit the highest activity with the 1X2J target protein. Beside, The interaction modes between studied ligand and the Target Proteinsfigure ,as shown in tables 3.8-3.13, the binding poses of Pt(F_2dpb)Cl, Pt(Fdpb)Cl, PlatinumCl, and PlatinumI complexes with 1XNJ target protein are given in Figure 3.6.

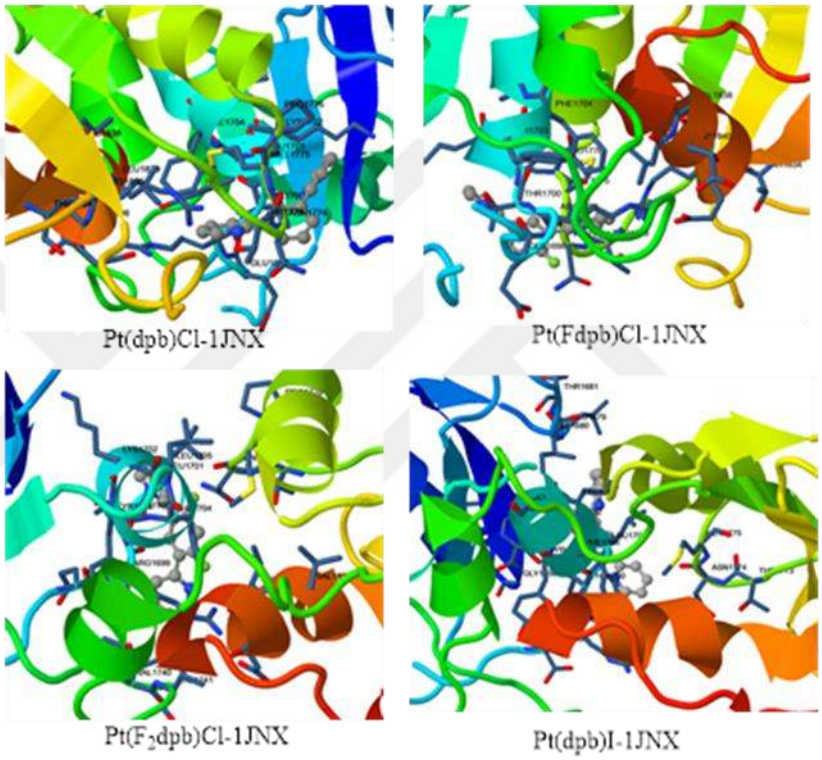

Figure 3.6. The Binding Modes of PlatinumCl, Pt(Fdpb)Cl, Pt(F2dpb)Cl, and PlatinumI with 1JNX

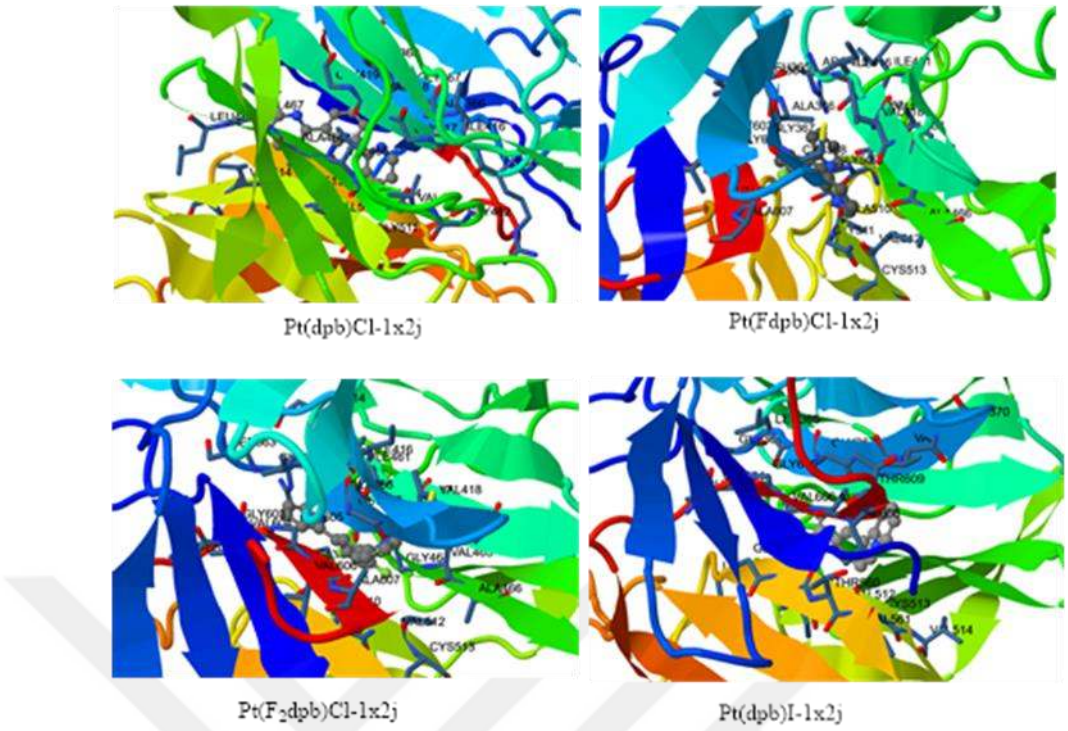

Figure 3.7. The binding modes of PlatinumCl, Pt(Fdpb)Cl, Pt(F2dpb)Cl, and PlatinumI with 1X2J

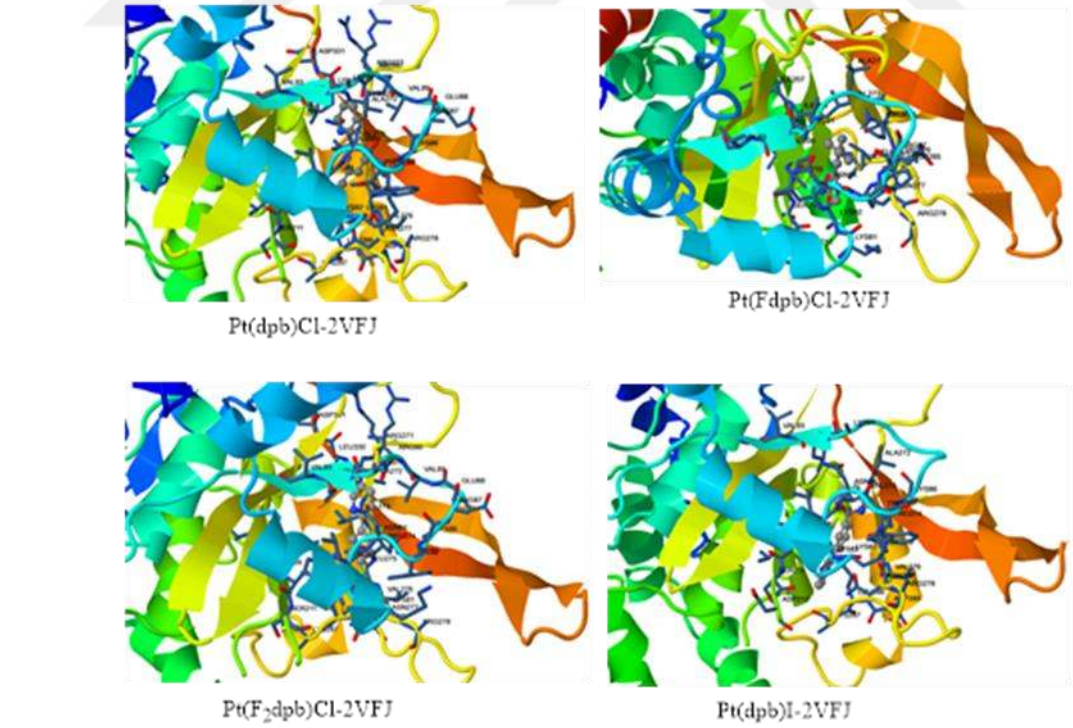

Figure 3.8. The binding modes of PlatinumCl, Pt(Fdpb)Cl, Pt(F2dpb)Cl, and PlatinumI with 2VFJ

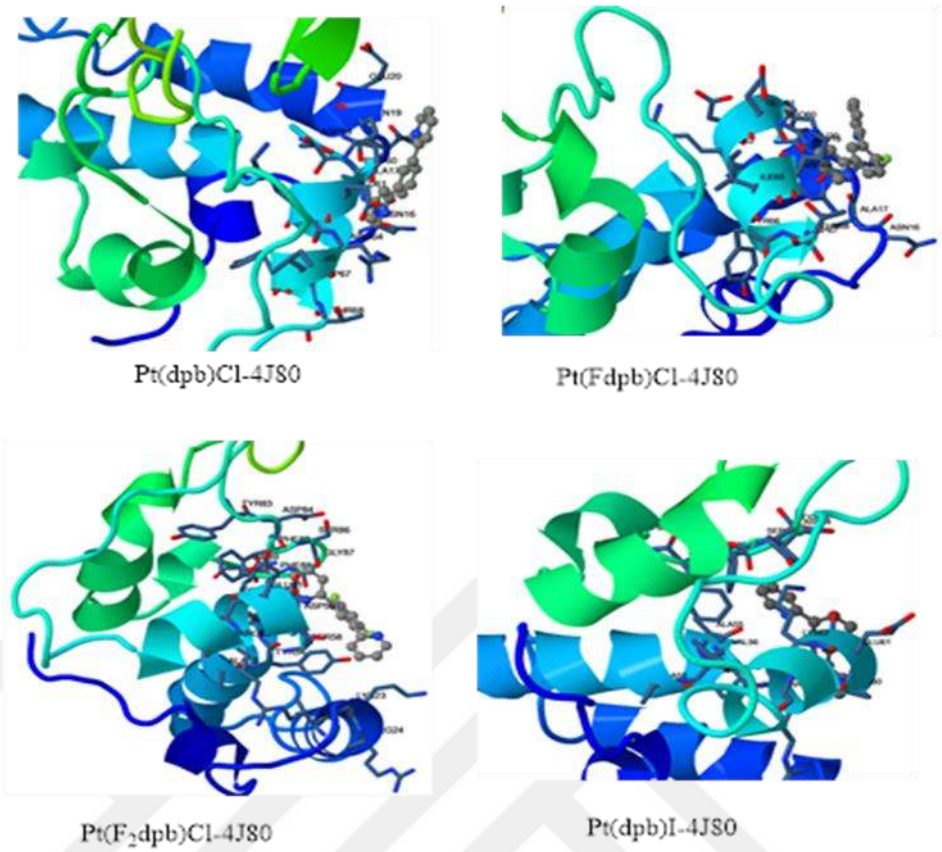

Figure 3.9. The binding modes of PlatinumCl, Pt(Fdpb)Cl, Pt(F2dpb)Cl, and PlatinumI with 4J80

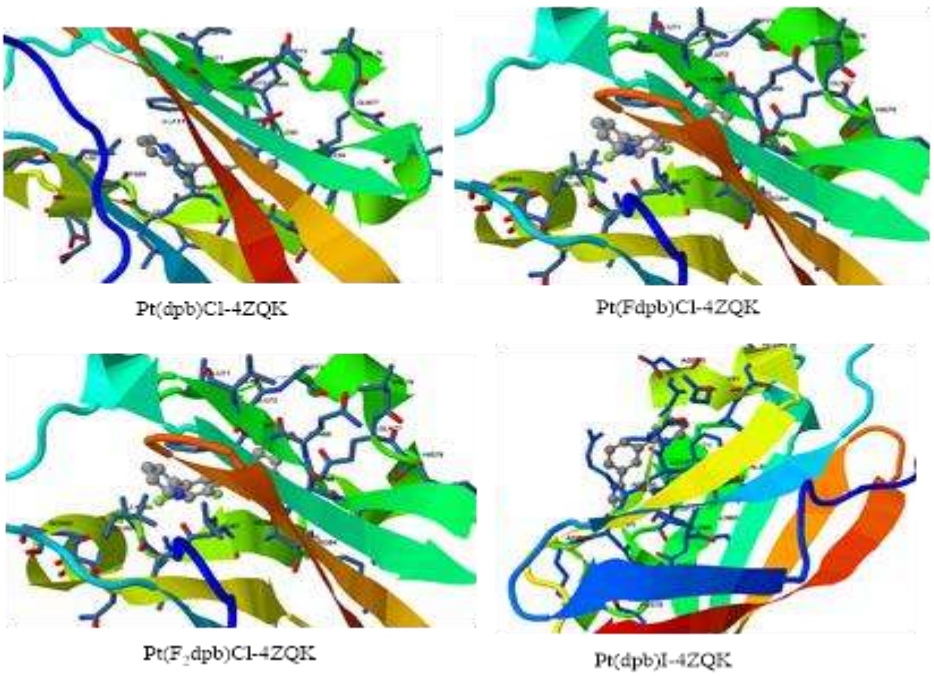

Figure 3.10. The binding modes of PlatinumCl, Pt(Fdpb)Cl, Pt(F2dpb)Cl, and PlatinumI with 4ZQK.

Table 3.8. The interaction modes between studied ligand and the selected 1JNX

Complex	H-bond	Polar	Hydrophobic	pi-pi	Halogen-bond
PlatinumCl	LEU1701 MET1775 LEU1839	-	-	PHE1704	-
Pt(Fdpb)Cl	LEU1701 MET1775 LEU1839	-		PHE1704	ARG1699
Pt(F_2dpb)Cl	-	ARG1699	VAL1740 MET1775	PHE1704	ASN1774
PlatinumI			ILE1680 LEU1701 LEU1705	-	-

Table 3.9. The interaction modes between studied ligand and the selected 2VFJ

Complex	H-bond	Polar	Hydrophobic	pi-pi	Halogen-bond
PlatinumCl	LYS82 ALA272 ASN277	-	VAL89 LEU92 ILE208 ILE210 VAL273 PRO274 LEU286 LEU330	TRP85	-
Pt(Fdpb)Cl	LYS82 LEU83	TRP85	LEU92 ILE210	-	PRO274
Pt(F_2dpb)Cl	GLY101 ASN189 LEU191	ARG123 TYR252	CYS103 LEU104 MET105 LEU191 ILE196 VAL229	TYR252 PHE257	GLY101 TYR252 HIS255
PlatinumI	LYS82 ASN277	-	LEU92 ILE208 ILE210 VAL273 PRO274 LEU286	-	-

Table 3.10. The interaction modes between studied ligand and the selected 1X2J

Complex	H-bond	Polar	Hydrophobic	pi-pi	Halogen-bond
PlatinumCl	-	-	VAL89 LEU83 ILE210 VAL273 PRO274	ASN84 TRP85	-
Pt(Fdpb)Cl	VAL512	-	CYS513 VAL561	-	VAL418
Pt(F_2dpb)Cl	GLY367 ILE416 VAL418	-	ALA366	-	LEU365 GLY3 VAL604 VAL606
PlatinumI	VAL512	-	ALA466 CYS513 VAL514 ILE559 VAL561	-	-

Table 3.11. The interaction modes between studied ligand and the selected 4J80

Complex	H-bond	Polar	Hydrophobic	pi-pi	Halogen-bond
PlatinumCl	-	ARG63	PRO60	-	-
Pt(Fdpb)Cl	ARG63	-	-	-	-
Pt(F_2dpb)Cl	SER58	TYR54	-	TYR54 PHE88	TYR54 SER86
PlatinumI	SER58	SER58 ASP59 LYS62	-	PHE85 PHE88	-

Table 3.12. The interaction modes between studied ligand and the selected 4ZQK

Complex	H-bond	Polar	Hydrophobic	pi-pi	Halogen-bond
PlatinumCl	ALA85	ARG86	ILE65 LEU87 LEU92	PHE67	-
Pt(Fdpb)Cl	-	-	LEU87	PHE67	LEU87
Pt(F_2dpb)Cl	LEU87	-	ILE65 LEU87 LEU92	PHE67	LEU87
PlatinumI	LEU87	-	ILE65 LEU87 LEU92	PHE67	-

3.6. OLED Properties

Many materials such as organic light-emitting diodes (OLEDs) can be designed with computational chemistry methods. In theory, compounds used in OLED structure can be classified as electron-transporting layers (ETL), hole-transporting layers (HTL), and emissive layers (EL) [97,98]. Also, there have been an electron injection layer (EIL), electron blocking layer (EBL), hole injection layer (HIL), and hole blocking layer (HBL) between cathode and anode.

Charge transfer is a very important parameter to explain the charge bearing property of the molecule in various biological and chemical reactions [99]. Interactions between conjugated pi-systems play an important role in different events like the stabilization of double-stranded DNA structure, protein folding, molecular recognition, and drug design [100]. These interactions may be of interest in the technological importance of (bio) molecular devices [101-104]. It is especially important for radiotherapy and chemotherapy tools. One of the main parameters considered in this context is named as transfer integral parameter and defined with "t" notation and is a simple semi-classical formulation of charge carrier mobility. "t" is directly related to frontier molecular orbitals due to intermolecular interactions [105]. The transfer integral parameter contains two different combinations. The parameters t_e is electron transfer integral and t_h is defined as hole transfer integral. t_e is electron transfer integral and t_h is defined ad hole transfer integral parameters. All these parameters are calculated by the Koopmans theorem (KT) method according to the following equations.

$$t_h = \frac{1}{2}(E_{HOMO} - E_{HOMO-1}) \tag{3.1}$$

$$t_e = \frac{1}{2}(E_{LUMO+1} - E_{LUMO}) \tag{3.2}$$

To obtain the transfer integrals "t" parameters, the crystal data of the examined complexes are required. Therefore, t parameters of the complexes will not be examined in this study [106-108].

The charge transfer properties of a molecule can be studied with reorganization energies and Marcus charge transfer theory. The total reorganization energy of the molecule is equal to the sum of internal (λ_{int}) and external (λ_{ext}) reorganization energy. Reorganization energies [109], λ_e and λ_h transfer can be calculated by the following equations:

$$\lambda e = (E_0^- - E_-^-) + (E_-^0 - E_0^0) \tag{3.3}$$

$$\lambda h = (E_0^+ - E_+^+) + (E_+^0 - E_0^0) \tag{3.4}$$

where E_0^+ is the energy of the cation calculated with the optimized structure of the neutral molecule.

E_0^- is the energy of the anion calculated with the optimized structure of the neutral molecule. E_+^+ and E_-^- are the energy of the cation and anion, respectively. E_+^0 is the energy of the neutral molecule calculated at the cationic state. (E_-^0) is the energy of the neutral molecule calculated at the anionic state. E_0^0 is the energy of the neutral molecule at the ground state. With these parameters, the charge transfer rates can be calculated with the Marcus theory.

$$K = t^2 \frac{2\pi}{\hbar} \frac{1}{\sqrt{4\pi\lambda k_B T}} exp\left[-\frac{(\lambda+\Delta G^0)^2}{4\lambda k_B T}\right] \tag{3.5}$$

where T is the temperature, k_B is the Boltzmann constant. ΔG° is the free energy of the hole transfer reaction (which is zero in the case of a transfer of holes between identical molecules).

In addition, two basic parameters are examined in EIL and HIL materials that determine the ease of charge transfer. These parameters are ionization potentials (IPs) and electron affinities (EAs). Fundamentally, lower IP and higher EA mean better hole and electron transport. In other words, smaller IP (larger EA) indicate easier injection of holes from the transport layer of the holes (electrons) to the emitter layers [110]. Ionization potential (IP_a), vertical ionization potential (IP_v), adiabatic electron affinity (EA_a), and vertical electron affinity (EA_v) are calculated as follows.

$$IP_a = E_+ - E_0^0 \tag{3.6}$$

$$IP_v = E_0^+ - E_0^0 \tag{3.7}$$

$$EA_a = E_0^0 - E_- \tag{3.8}$$

$$EA_v = E_0^0 - E_0^- \tag{3.9}$$

Here, E_0^- (E_0^+) is the energy of the anion calculated with the optimized structure of the neutral molecule. $E_-(E_+)$ is the energy of the anion calculated with the optimized anion structure [111]. The calculated values of the reorganization energy, the adiabatic and vertical ionization potentials (IP_a/IP_v), and electron affinities (EA_a/EA_v) (in eV) for the complexes examined are listed in Table 4.13.

Table 3.13. The adiabatic and (IPa/IPv) and (EAa/EAv) (in eV) for the platinum complexes

Complex	**IP_a**	**IP_v**	**EA_a**	**EA_v**	**λ_e**	**λ_h**
PlatinumCl	0.2739	0.2799	0.0319	0.0267	0.18	0.15
Pt(Fdpb)Cl	0.2815	0.3088	0.0372	0.0312	0.18	0.18
Pt(F_2dpb)Cl	0.2889	0.2958	0.0401	0.0327	0.16	0.13
PlatinumI	0.2633	0.2909	0.0354	0.0301	0.17	0.10

In literature, the Alq3 and TPD compounds as the typical ETL and HTL materials have been used as a comparison substance and its electron reorganization energy of Alq3 at 0.276 eV [112] and the hole reorganization energy of TPD at 0.290 eV were reported in detail [113].

The electron and hole reorganization energies of the PlatinumCl, Pt(Fdpb)Cl, Pt(F_2dpb)Cl and PlatinumI complexes are calculated at 0.18, 0.18, 0.16, 0.17 and 0.15, 0.18, 0.13, 0.10 eV, respectively. In that case, the platinum complexes may be a suitable ETL molecule because its λe values are smaller than that of Alq3. Furthermore, it is seen that the λ_h values of the platinum complexes are considerably smaller than that of TPD. Because of that, it can also be a perfect HTL material.

Besides, according to the data in Table 4.13, PlatinumCl, Pt(Fdpb)Cl, Pt(F_2dpb)Cl and PlatinumI complexes examined have the lowest IP and EA values in the gas phase. EA values are not high. Therefore, platinum complexes are considered to be an excellent material for HIL.

4. CONCLUSIONS

Pt(F_2dpb)Cl, Pt(Fdpb)Cl, PlatinumCl, and PlatinumI complexes were optimized with HF and DFT (B3LYP and M062X) methods in combining with CEP-4G, CEP-31G, CEP-12G, LANL2DZ, LANL2MB, and SDD basis sets. According to the determined coefficient of R^2, it was found that M062X/CEP-31G is the best level. FTIR and ^{13}C-NMR spectroscopic values of studied complexes obtained and interpreted in detail. Platinum complexes, which are important with their anti-cancer properties were docked with molecular simulation against breast, ovarian, colon, pancreatic, lung, and melanoma cancer cell lines. The investigated complexes showed the highest inhibitory activity against the breast cancer cell line. We concluded that, after evaluating all theoretical results, the title complexes can be considered as an anticancer drug. Finally, the investigated complexes found to be a good candidate for ETL, HTL, and HIL material.

REFERENCES

[1] Kaya C., (2008). Inorganic Chemistry I, *Palme Publishing*, Ankara,

[2] Dolmans, D. E., Fukumura, D., & Jain, R. K. (2003). Photodynamic therapy for cancer. *Nature reviews cancer*, 3(5), 380-387.

[3] Wilson, B. C. (1970). Photodynamic therapy for cancer: principles. *Canadian journal of gastroenterology,* 16.

[4] Vrouenraets, M. B., Visser, G. W., & Snow, G. B. (2003). Basic principles, applications in oncology, and improved selectivity of photodynamic therapy. *Anticancer Research*, 23(1B), 505-522.

[5] Dougherty, T. J., Gomer, C. J., Henderson, B. W., Jori, G., Kessel, D., Korbelik, M., ... & Peng, Q. (1998). Photodynamic therapy. JNCI: *Journal of the national cancer institute*, 90(12), 889-905.

[6] Gudgin, E. D., Goyan, R. L., & Pottier, R. H. (2002). New directions in photodynamic therapy. *Cellular and molecular biology* (Noisy-le-Grand, France), 48(8), 939-954.

[7] https://www.cancer.gov/about-cancer/treatment/types/surgery/photodynamic-fact-sheet Access: January 2020

[8] Dolmans, D. E., Fukumura, D., & Jain, R. K. (2003). Photodynamic therapy for cancer. *Nature reviews cancer,* 3(5), 380-387.

[9] Zhao, Y., & Truhlar, D. G. (2008). The M06 suite of density functionals for main group thermochemistry, thermochemical kinetics, noncovalent interactions, excited states, and transition elements: two new functionals and systematic testing of four M06-class functionals and 12 other functionals. *Theoretical Chemistry Accounts*, 120(1-3), 215-241.

[10] Shaili, E. (2014). Platinum anticancer drugs and photochemotherapeutic agents: recent advances and future developments. *Science progress*, 97(1), 20-40.

[11] Takahara, P. M., Frederick, C. A., & Lippard, S. J. (1996). Crystal structure of the anticancer drug cisplatin bound to duplex DNA. *Journal of the American Chemical Society*, 118(49), 12309-12321.

[12] Takahara, P. M., Rosenzweig, A. C., Frederick, C. A., & Lippard, S. J. (1995). Crystal structure of double-stranded DNA containing the major adduct of the anticancer drug cisplatin. *Nature*, 377(6550), 649-652.

[13] Silverman, A. P., Bu, W., Cohen, S. M., & Lippard, S. J. (2002). 2.4-Å Crystal structure of the asymmetric platinum complex {Pt (ammine)(cyclohexylamine)} 2+ bound to a dodecamer DNA duplex. *Journal of Biological Chemistry*, 277(51), 49743-49749.

[14] Gelasco, A., & Lippard, S. J. (1998). NMR solution structure of a DNA dodecamer duplex containing a cis-diammineplatinum (II) d (GpG) intrastrand cross-link, the major adducts of the anticancer drug cisplatin. *Biochemistry*, 37(26), 9230-9239.

[15] Esteban-Fernández, D., Montes-Bayón, M., González, E. B., Gomez, M. G., Palacios, M. A., & Sanz-Medel, A. (2008). Atomic (HPLC-ICP-MS) and molecular mass spectrometry (ESI-Q-TOF) to study cis-platin interactions with serum proteins. *Journal of Analytical Atomic Spectrometry,* 23(3), 378-384.

[16] Michalke, B. (2010). Platinum speciation used for elucidating activation or inhibition of Pt-containing anti-cancer drugs. *Journal of Trace Elements in Medicine and Biology*, 24(2), 69-77.

[17] Çal, A. (2014). Investigation of New Generation Platinum Complexes by Mass Spectrometric Methods and Investigation of Anticancer Activities in In Vitro. Ph.D. Thesis, *Chemistry*

Department, Institute of Science, Hacettepe University.

[18] McNaught, A. D. (1997). Compendium of chemical terminology (Vol. 1669). *Oxford: Blackwell Science.*

[19] Allisy-Roberts, P., & Williams, J. (2008). Radiation physics. *Farr's Physics for Medical Imaging,* 1–21.

[20] Peyratout, C. S., Aldridge, T. K., Crites, D. K., & McMillin, D. R. (1995). DNA-binding studies of a bifunctional platinum complex that is a luminescent intercalator. *Inorganic Chemistry*, 34(17), 4484-4489.

[21] Maruyama, T., & Yamamoto, T. (1997). Effective Photocatalytic System Based on Chelating π-Conjugated Poly (2, 2 '-bipyridine-5, 5 '-diyl) and Platinum for Photoevolution of H2 from Aqueous Media and Spectroscopic Analysis of the Catalyst. *The Journal of Physical Chemistry* B, 101(19), 3806-3810.

[22] Roundhill, D. M., Gray, H. B., & Che, C. M. (1989). Pyrophosphito-bridged diplatinum chemistry. *Accounts of Chemical Research*, 22(2), 55-61.

[23] Nocera, D. G. (1995). Chemistry of the multielectron excited state. *Accounts of chemical research*, 28(5), 209-217.

[24] Fischer, T., Czerwieniec, R., Hofbeck, T., Osminina, M. M., & Yersin, H. (2010). Triplet state properties of a red light emitting [Pt (s-thpy)(acac)] compound. *Chemical Physics Letters*, 486(1-3), 53-59.

[25] Baldo, M., Lamansky, S., Burrows, P., Thompson, M., & Forrest, S. (1999). Very high-efficiency green organic light-emitting devices based on electrophosphorescence. *Applied Physics Letters,* 75(1), 4-6.

[26] Baldo, M. A., O'Brien, D. F., You, Y., Shoustikov, A., Sibley, S., Thompson, M. E., & Forrest, S. R. (1998). Highly efficient phosphorescent emission from organic electroluminescent devices. *Nature,* 395(6698), 151-154.

[27] Baitalik, S., Wang, X. Y., & Schmehl, R. H. (2004). A trimetallic mixed Ru (II)/Fe (II) terpyridyl complex with a long-lived excited state in solution at room temperature. *Journal of the American Chemical Society,* 126(50), 16304-16305.

[28] Ciofini, I., Lainé, P. P., Bedioui, F., & Adamo, C. (2004). Photoinduced intramolecular electron transfer in ruthenium and osmium polyads: Insights from theory. *Journal of the American Chemical Society,* 126(34), 10763-10777.

[29] Wong, W. Y., & Ho, C. L. (2009). Heavy metal organometallic electrophosphors derived from multi-component chromophores. *Coordination Chemistry Reviews*, 253(13-14), 1709-1758.

[30] Sato, T., Awano, H., Haba, O., Katagiri, H., Pu, Y. J., Takahashi, T., & Yonetake, K. (2012). Synthesis, characterization, and polarized luminescence properties of platinum (II) complexes having a rod-like ligand. *Dalton Transactions*, 41(27), 8379-8389.

[31] Brooks, J., Babayan, Y., Lamansky, S., Djurovich, P. I., Tsyba, I., Bau, R., & Thompson, M. E. (2002). Synthesis and characterization of phosphorescent cyclometalated platinum complexes. *Inorganic Chemistry,* 41(12), 3055-3066.

[32] Puttock, E. V., Walden, M. T., & Williams, J. G. (2018). The luminescence properties of multinuclear platinum complexes. *Coordination Chemistry Reviews*, 367, 127-162.

[33] Sato, T., Awano, H., Haba, O., Katagiri, H., Pu, Y. J., Takahashi, T., & Yonetake, K. (2012). Synthesis, characterization, and polarized luminescence properties of platinum (II) complexes having a rod-like ligand. *Dalton Transactions*, 41(27), 8379-8389.

[34] Lowe, J. A., Stacey, O. J., Horton, P. N., Coles, S. J., & Pope, S. J. (2016). Alkyl chain functionalised, cyclometalated platinum (II) complexes: Syntheses, luminescence properties and X-ray crystal structure. *Journal of Organometallic Chemistry*, 805, 87-93.

[35] Kamtekar, K. T., Monkman, A. P., & Bryce, M. R. (2010). Recent advances in white organic light-emitting materials and devices (WOLEDs). *Advanced Materials*, 22(5), 572-582.

[36] D'Andrade, B. W., & Forrest, S. R. (2004). White organic light-emitting devices for solid-state lighting. *Advanced Materials*, 16(18), 1585-1595.

[37] Kim, J. H., Triambulo, R. E., & Park, J. W. (2017). Effects of the interfacial charge injection properties of silver nanowire transparent conductive electrodes on the performance of organic light-emitting diodes. *Journal of Applied Physics*, 121(10), 105304.

[39] Sharma, R. K., Katiyar, M., Rao, I. K., & Unni, K. N. (2016). Effect of the electric field during annealing of organic light emitting diodes for improving its on/off ratio. *Physical Chemistry Chemical Physics,* 18(4), 2747-2755.

[40] Wei, Q., Ge, Z., & Voit, B. (2019). Thermally activated delayed fluorescent polymers: structures, properties, and applications in OLED devices. *Macromolecular rapid communications*, 40(1), 1800570.

[41] Shangguan, R., Mu, G., Wang, L., Zhuang, S., & Chen, C. H. (2015). Comparative study of using different alkali metal alkylcarboxylates as electron injection materials in OLEDs. *Journal of Materials Chemistry* C, 3(26), 6916-6923.

[42] Üngördü, A. (2019). Charge transfer properties of Gaq3 and its derivatives: An OLED study. *Chemical Physics Letters*, 733, 136696.

[43] Zou, S. J., Shen, Y., Xie, F., Chen, J. D., Li, Y., & Tang, J. (2020). Recent Advances in Organic Light-Emitting Diodes: Toward Smart Lighting and Displays. *Materials Chemistry Frontiers*.

[44] Lim, J. S., & Shin, P. K. (2007). Improved performance of organic light-emitting devices with plasma treated ITO surface and plasma polymerized methyl methacrylate buffer layer. *Applied surface science,* 253(8), 3828-3833.

[45] Havare, A. K., Can, M., Tozlu, C., Kus, M., Okur, S., Demic, Ş., ... & Icli, S. (2016). Charge transfer through amino groups-small molecules interface improving the performance of electroluminescent devices. *Optical Materials*, 55, 94-101.

[46] Murata, H., Mattoussi, H., Merritt, C. D., Iizumi, Y., Kido, J., Tokuhisa, H., ... & Kafafi, Z. H. (2000). Molecular organic light-emitting diodes based on a guest-host active layer: Approaches for enhancing device performance. *Molecular Crystals and Liquid Crystals Science and Technology. Section A. Molecular Crystals and Liquid Crystals*, 353(1), 567-580.

[47] Yamamori, A., Adachi, C., Koyama, T., & Taniguchi, Y. (1999). Electroluminescence of organic light emitting diodes with a thick hole transport layer composed of a triphenylamine based polymer doped with an antimonium compound. *Journal of applied physics*, 86(8), 4369-4376.

[48] Kubicki, J. D., & Mueller, K. T. (2010). Computational spectroscopy in environmental chemistry. In Computational Spectroscopy: Methods, Experiments and Applications (pp. 323-351). John Wiley and Sons.

[49] Wong, M. W. (1996). Vibrational frequency prediction using density functional theory. *Chemical Physics Letters*, 256(4-5), 391-399.

[50] Andersson, M. P., & Uvdal, P. (2005). New scale factors for harmonic vibrational frequencies using the B3LYP density functional method with the triple-ζ basis set 6-311+ G (d, p). *The Journal of*

Physical Chemistry A, 109(12), 2937-2941.

[51] Kaiser, E., Simpson, A. J., Dria, K. J., Sulzberger, B., & Hatcher, P. G. (2003). Solid-state and multidimensional solution-state NMR of solid phase extracted and ultrafiltered riverine dissolved organic matter. *Environmental science & technology*, 37(13), 2929-2935.

[52] Diallo, M. S., Simpson, A., Gassman, P., Faulon, J. L., Johnson, J. H., Goddard, W. A., & Hatcher, P. G. (2003). 3-D structural modeling of humic acids through experimental characterization, computer assisted structure elucidation and atomistic simulations. 1. Chelsea soil humic acid. *Environmental science & technology*, 37(9), 1783-1793.

[53] Simpson, A. J., Kingery, W. L., & Hatcher, P. G. (2003). The identification of plant derived structures in humic materials using three-dimensional NMR spectroscopy. *Environmental science & technology,* 37(2), 337-342.

[54] Cody, G. D., Mysen, B., Sághi-Szabó, G., & Tossell, J. A. (2001). Silicate-phosphate interactions in silicate glasses and melts: I. A multinuclear (27Al, 29Si, 31P) MAS NMR and ab initio chemical shielding (31P) study of phosphorous speciation in silicate glasses. *Geochimica et Cosmochimica Acta*, 65(14), 2395-2411.

[55] Tossell, J. A. (2006). Boric acid adsorption on humic acids: ab initio calculation of structures, stabilities, 11B NMR and 11B, 10B isotopic fractionations of surface complexes. *Geochimica et cosmochimica acta,* 70(20), 5089-5103.

[56] Marcus, R. A. (1956). On the theory of oxidation-reduction reactions involving electron transfer. I. *The Journal of chemical physics*, 24(5), 966-978.

[57] Uratani, H., Kubo, S., Shizu, K., Suzuki, F., Fukushima, T., & Kaji, H. (2016). Detailed analysis of charge transport in amorphous organic thin layer by multiscale simulation without any adjustable parameters. *Scientific reports*, 6, 39128.

[58] Melander, M., Jónsson, E. O., Mortensen, J. J., Vegge, T., & García Lastra, J. M. (2016). Implementation of constrained DFT for computing charge transfer rates within the projector augmented wave method. *Journal of chemical theory and computation,* 12(11), 5367-5378.

[59] Trasobares, J., Rech, J., Jonckheere, T., Martin, T., Alévêque, O., Levillain, E., ... & Sivakumarasamy, R. (2017). Estimation of π–π electronic couplings from current measurements. *Nano Letters*, 17(5), 3215-3224.

[60] Gillet, N., Berstis, L., Wu, X., Gajdos, F., Heck, A., de la Lande, A., ... & Elstner, M. (2016). Electronic coupling calculations for bridge-mediated charge transfer using constrained density functional theory (CDFT) and effective hamiltonian approaches at the density functional theory (DFT) and fragment-orbital density functional tight binding (FODFTB) level. *Journal of chemical theory and computation,* 12(10), 4793-4805.

[61] Irfan, A. (2014). Modeling of efficient charge transfer materials of 4, 6-di (thiophen-2-yl) pyrimidine derivatives: Quantum chemical investigations. *Computational materials science,* 81, 488-492.

[62] Bugg TD (2004). Introduction to Enzyme and Coenzyme Chemistry (PDF) (2nd ed.). *Blackwell Publishing Limited.*

[63] Foresman J. B., Frisch E., (1993). Exploring Chemistry With Electronic Structure Methods, Sec. Ed., *Gaussian Inc.*

[64] Hohenberg P., Kohn W., (1964). Phys. Rev., 136, 864.

[65] Kohn W., Sham L. J., (1965). Phys. Rev., 140, 1133.

[66] Erkan S., (2012). The Calculation of Structural Parameters And Stretching Frequencies Of Dicobalt Octacarbonyl Isomers By Using Ab Initio Molecular Orbital Methods Master's Thesis, Science

Faculty, *Inorganic Chemistry Department, Cumhuriyet University.*

[67] https://en.wikipedia.org/wiki/Basis_set_(chemistry) Access Date : October 2019.

[68] Becke A. D., (1993). A new mixing of Hartree-Fock and local density-functional teories, J. *Chem. Phys.*, 98, 2, 1372-1378.

[69] Davidson, Ernest; Feller, David (1986). "Basis set selection for molecular calculations*". Chem. Rev.* 86 (4): 681–696

[70] Çiçek, E. (2016). Theoretical investigation of the binding properties of some hydroxamic acid derivatives which are histone deacetylase (HDAC) inhibitors by molecular clamping method *(Doctoral dissertation, Recep Tayyip Erdoğan University / Institute of Science / Chemistry Department).*

[71] Ritchie, D. Hex 8.0. 0 user manual, 1996.

[72] Zhao, Y., & Truhlar, D. G. (2008). The M06 suite of density functionals for main group thermochemistry, thermochemical kinetics, noncovalent interactions, excited states, and transition elements: two new functionals and systematic testing of four M06-class functionals and 12 other functionals. *Theoretical Chemistry Accounts*, 120(1-3), 215-241.

[73] Gao, H. (2011). Theoretical studies of molecular structures and properties of platinum (II) antitumor drugs. Spectrochimica Acta - Part A: Molecular and Biomolecular Spectroscopy. 79, 687-693.

[74] Iwakiri, A., Konno, Y., & Shinozaki, K. (2019). Determination of excimer emission quantum yield of Pt (dpb) Cl (dpbH= 1, 3-di (2-pyridyl) benzene and its analogues in solution. *Journal of Luminescence,* 207, 482-490.

[75] Sathyanarayana, D.N., (2015). Vibrational spectroscopy: theory and applications, *New Age International.*

[76] Varsányi, G., (1974). Assignments for vibrational spectra of seven hundred benzene derivatives, *Halsted Press.*

[77] Mohan, J., (2004). Organic spectroscopy: principles and applications, *Alpha Science Int'l Ltd*.

[78] Lorenc, J., (2012). Dimeric structure and hydrogen bonds in 2-N-ethylamino-5-metyl-4-nitro-pyridine studied by XRD, IR and Raman methods and DFT calculations, *Vibrational Spectroscopy,* 61, 112-123.

[79] Sharma, Y., (2009). Elementary organic spectroscopy, principles and chemical application*, Chand and Company Ltd, New Delhi, India.*

[80] Ramachandran, S. and Velraj, G., (2012). FT-IR, FT-Raman spectral analysis and density functional theory calculations studies of 3-chloro-2-nitrobenzyl alcohol, *Rom. Journ. Phys*, 57(7-8), 1128-1137.

[81] Abkowicz-Bienko, A., Bienko, D., and Latajka, Z., (2000). Density functional studies on the two conformers of 2-fluoro-4, 6-dinitrophenol: vibrational assignment based on potential energy distribution*, Journal of Molecular Structure*, 552(1-3), 165-175.

[82] Ardyukoiva, T. (1973)., Atlas of Spectra of Aromatic and Heterocyclic Compounds, *Nauka Sib otd, Novosibirsk.*

[83] Varsányi, G., (2012). Vibrational spectra of benzene derivatives, *Elsevier.*

[84] Krishnakumar, V., Surumbarkuzhali, N., and Muthunatesan, S., (2009). Scaled quantum chemical studies on the vibrational spectra of 4-bromo benzonitrile, *Spectrochimica Acta Part A: Molecular*

and Biomolecular Spectroscopy, 71(5), 1810-1813.

[85] Fleming, G.D., Koch, R., and Vallette, M.C., (2006). Theoretical study of the syn and anti thiophene-2-aldehyde conformers using density functional theory and normal coordinate analysis, *Spectrochimica Acta Part A: Molecular and Biomolecular Spectroscopy*, 65(3-4), 935-945.

[86] Ünal, A. and Eren, B., (2013). FT-IR, dispersive Raman, NMR, DFT and antimicrobial activity studies on 2-(Thiophen-2-yl)-1H-benzo [d] imidazole, Spectrochimica Acta Part A: *Molecular and Biomolecular Spectroscopy*, 114, 129-136.

[87] Badawi, H.M., (2009). Structural stability, C–N internal rotations and vibrational spectral analysis of non-planar phenylurea and phenylthiourea, *Spectrochimica Acta Part A: Molecular and Biomolecular Spectroscopy,* 72(3), 523-527.

[88] Knicker, H., Almendros, G., González-Vila, F.J., Lüdemann, H.-D., and Martin, F., (1995). 13C and 15N NMR analysis of some fungal melanins in comparison with soil organic matter, *Organic Geochemistry*, 23(11-12), 1023-1028.

[89] Cheeseman, J.R., Trucks, G.W., Keith, T.A., and Frisch, M.J., (1996). A comparison of models for calculating nuclear magnetic resonance shielding tensors, *The Journal of chemical physics,* 104(14), 5497-5509.

[90] Frisch, M., Trucks, G., Schlegel, H., Scuseria, G., Robb, M., Cheeseman, J., Zakrzewski, V., Montgomery Jr, J., Stratmann, R.E., and Burant, J., (1998). Gaussian 98, revision a. 7, Gaussian, Inc., Pittsburgh, PA, 12.

[91] Erkan, S., Kaya, S., Sayin, K., & Karakaş, D. (2020). Structural, spectral characterization and molecular docking analyses of mer-ruthenium (II) complexes containing the bidentate chelating ligands. *Spectrochimica Acta Part A: Molecular and Biomolecular Spectroscopy*, 224, 117399.

[92] Williams, R. S., Green, R., & Glover, J. M. (2001). Crystal structure of the BRCT repeat region from the breast cancer-associated protein BRCA1. *Nature structural biology*, 8(10), 838-842.

[93] Padmanabhan, B., Tong, K. I., Ohta, T., Nakamura, Y., Scharlock, M., Ohtsuji, M., ... & Yamamoto, M. (2006). Structural basis for defects of Keap1 activity provoked by its point mutations in lung cancer. *Molecular cell,* 21(5), 689-700.

[94] Komander, D., & Barford, D. (2008). Structure of the A20 OTU domain and mechanistic insights into deubiquitination. *Biochemical Journal*, 409(1), 77-85.

[95] Barends, T. R., Brosi, R. W., Steinmetz, A., Scherer, A., Hartmann, E., Eschenbach, J., ... & Bittl, R. (2013). Combining crystallography and EPR: crystal and solution structures of the multidomain cochaperone DnaJ. *Acta Crystallographica Section D: Biological Crystallography*, 69(8), 1540-1552.

[96] Zak, K. M., Kitel, R., Przetocka, S., Golik, P., Guzik, K., Musielak, B., ... & Holak, T. A. (2015). Structure of the complex of human programmed death 1, PD-1, and its ligand PD-L1. *Structure,* 23(12), 2341-2348.

[97] Kim, J. H., Triambulo, R. E., & Park, J. W. (2017). Effects of the interfacial charge injection properties of silver nanowire transparent conductive electrodes on the performance of organic light-emitting diodes. *Journal of Applied Physics*, 121(10), 105304.

[98] Zhao, J., Chen, X., Yang, Z., Liu, T., Yang, Z., Zhang, Y., ... & Chi, Z. (2018). Highly-efficient doped and nondoped organic light-emitting diodes with external quantum efficiencies over 20% from a multifunctional green thermally activated delayed fluorescence emitter. *The Journal of Physical Chemistry* C, 123(2), 1015-1020.

[99] Melander, M., Jónsson, E. O., Mortensen, J. J., Vegge, T., & García Lastra, J. M. (2016).

Implementation of constrained DFT for computing charge transfer rates within the projector augmented wave method. *Journal of chemical theory and computation*, 12(11), 5367-5378.

[100] Erkan, S. (2019). Activity of the rocuronium molecule and its derivatives: A theoretical calculation. *Journal of Molecular Structure*, 1189, 257-264.

[101] Wu, S., González, M. T., Huber, R., Grunder, S., Mayor, M., Schönenberger, C., & Calame, M. (2008). Molecular junctions based on aromatic coupling. *Nature nanotechnology*, 3(9), 569.

[102] Nerngchamnong, N., Yuan, L., Qi, D. C., Li, J., Thompson, D., & Nijhuis, C. A. (2013). The role of van der Waals forces in the performance of molecular diodes. *Nature nanotechnology*, 8(2), 113.

[103] Venkataraman, L., Klare, J. E., Nuckolls, C., Hybertsen, M. S., & Steigerwald, M. L. (2006). Dependence of single-molecule junction conductance on molecular conformation. *Nature,* 442(7105), 904-907.

[104] Cheng, Z. L., Skouta, R., Vazquez, H., Widawsky, J. R., Schneebeli, S., Chen, W., ... & Venkataraman, L. (2011). In situ formation of highly conducting covalent Au–C contacts for single-molecule junctions. *Nature nanotechnology*, 6(6), 353.

[105] Cornil, J., Beljonne, D., Calbert, J. P., & Brédas, J. L. (2001). Interchain interactions in organic π-conjugated materials: impact on electronic structure, optical response, and charge transport. *Advanced materials,* 13(14), 1053-1067.

[106] Wen, S. H., Li, A., Song, J., Deng, W. Q., Han, K. L., & Goddard III, W. A. (2009). First-principles investigation of anistropic hole mobilities in organic semiconductors. *The Journal of Physical Chemistry* B, 113(26), 8813-8819.

[107] Chai, S., Wen, S. H., Huang, J. D., & Han, K. L. (2011). Density functional theory study on electron and hole transport properties of organic pentacene derivatives with electron-withdrawing substituent. *Journal of computational chemistry*, 32(15), 3218-3225.

[108] Deng, W. Q., Sun, L., Huang, J. D., Chai, S., Wen, S. H., & Han, K. L. (2015). Quantitative prediction of charge mobilities of π-stacked systems by first-principles simulation. *Nature protocols,* 10(4), 632.

[109] Stark, M. S. (1997). Epoxidation of alkenes by peroxyl radicals in the gas phase: structure− activity relationships. *The Journal of Physical Chemistry* A, 101(44), 8296-8301.

[110] Gao, J., Li, J., Li, X., Han, D., Guo, P., Zhu, X., & Shang, X. (2019). Theoretical investigation on the effect of the modification of 2-phenylpyridine ligand on the photophysical properties for a series of iridium (III) complexes with carbazate ancillary ligands. *Journal of Luminescence*, 209, 365-371.

[111] Üngördü, A. (2020). Electronic, optical, and charge transfer properties of porphyrin and metallated porphyrins in different media. *International Journal of Quantum Chemistry*, 120(6), e26128.

[112] Lukyanov, A., Lennartz, C., & Andrienko, D. (2009). Amorphous films of tris (8-hydroxyquinolinato) aluminium: Force-field, morphology, and charge transport. *physica status solidi (a)*, 206(12), 2737-2742.

[113] Gruhn, N. E., da Silva Filho, D. A., Bill, T. G., Malagoli, M., Coropceanu, V., Kahn, A., & Brédas, J. L. (2002). The vibrational reorganization energy in pentacene: molecular influences on charge transport. *Journal of the American Chemical Society*, 124(27), 7918-7919.

CURRICULUM VITAE

Hunar HAMA KHALID

PERSONAL INFORMATIONS

Birth of Place	**:** Sulaimani-Iraq
Birth of Date	**:** 27.10.1991
Nationalty	**:** Iraqi
Address	**:** Said Sadq as Sulaimani as Iraq
E-mail	**:** hunaranwar26@gmail.com
Languages	**:** Kurdish (Native), Turkish (B2), English (B2)

EDUCATION

Bachelor	**:** University of Sulaimanyeh, Faculty of Science, Department of Physics, 2014
High School	**:** Said Sadq as Sulaimaniyeh- Iraq, 2010

RESEARCH EXPERIENCES

- ✓ GaussView Software and Origin Lab Software

WORK EXPERIENCE

2014 – 2015: I had been working as a teacher for 4 months

2016 – 2018: I have been working as accountant in ANES Company